NASA TECHNICAL NOTE

NASA TN D-7441

NASA TN D-7441

ANALYTICAL STUDY OF TAKEOFF AND LANDING PERFORMANCE FOR A JET STOL TRANSPORT CONFIGURATION WITH FULL-SPAN, EXTERNALLY BLOWN, TRIPLE-SLOTTED FLAPS

by Harold P. Washington and John T. Gibbons

Flight Research Center
Edwards, Calif. 93523

NATIONAL AERONAUTICS AND SPACE ADMINISTRATION • WASHINGTON, D. C. • OCTOBER 1973

1. Report No.	2. Government Accession No.	3. Recipient's Catalog No.
NASA TN D-7441		

4. Title and Subtitle	5. Report Date
ANALYTICAL STUDY OF TAKEOFF AND LANDING PERFORMANCE FOR A JET STOL TRANSPORT CONFIGURATION WITH FULL-SPAN, EXTERNALLY BLOWN, TRIPLE-SLOTTED FLAPS	October 1973
	6. Performing Organization Code
7. Author(s)	8. Performing Organization Report No.
Harold P. Washington and John T. Gibbons	H-709
	10. Work Unit No.
9. Performing Organization Name and Address	769-89-01-00
NASA Flight Research Center P. O. Box 273 Edwards, California 93523	11. Contract or Grant No.
	13. Type of Report and Period Covered
12. Sponsoring Agency Name and Address	Technical Note
National Aeronautics and Space Administration Washington, D. C. 20546	14. Sponsoring Agency Code

15. Supplementary Notes

16. Abstract

Takeoff and landing performance characteristics and field length requirements were determined analytically for a jet STOL transport configuration with full-span, externally blown, triple-slotted flaps. The configuration had a high wing, high T-tail, and four pod-mounted high-bypass-ratio turbofan engines located under and forward of the wing. One takeoff and three approach and landing flap settings were evaluated. The effects of various parameters (i.e., wing loading, thrust-to-weight ratio, weight, ambient temperature, altitude) on takeoff and landing field length requirements are discussed.

17. Key Words (Suggested by Author(s))	18. Distribution Statement
Takeoff and landing Jet STOL aircraft Externally blown flaps	Unclassified - Unlimited

19. Security Classif. (of this report)	20. Security Classif. (of this page)	21. No. of Pages	22. Price*
Unclassified	Unclassified	47	Domestic, $3.00 Foreign, $5.50

* For sale by the National Technical Information Service, Springfield, Virginia 22151

ANALYTICAL STUDY OF TAKEOFF AND LANDING PERFORMANCE FOR A JET STOL TRANSPORT CONFIGURATION WITH FULL-SPAN, EXTERNALLY BLOWN, TRIPLE-SLOTTED FLAPS

Harold P. Washington and John T. Gibbons
Flight Research Center

SUMMARY

An analytical study was made to assess the takeoff and landing performance and field length requirements for a jet STOL transport configuration with full-span, externally blown, triple-slotted flaps. The 21,772-kilogram (48,000-pound-mass) baseline study configuration had a high wing, high T-tail, and four pod-mounted high-bypass-ratio turbofanjet engines located under and forward of the wing. The aerodynamic characteristics used were based on wind-tunnel data. One takeoff flap setting of 35° and three approach and landing flap settings of 40°, 50°, and 60° were evaluated. All takeoff and landing performance calculations were performed with a two-degree-of-freedom, point mass trajectory program.

Ground rules for performing short-field takeoff and landing maneuvers and for determining field length requirements were defined. Minimum speeds were calculated for both the all-engines-operating condition and the critical safe engine-out case. Operational margins were applied to develop operational envelopes for each flap setting. Takeoff and landing performance characteristics and field length requirements are presented, and time histories of typical short-field takeoff and landing maneuvers are included. A parametric study was also conducted to determine the effect on takeoff and landing field length requirements of variations in wing loading, thrust-to-weight ratio, weight, deceleration rate, delay, ambient temperature, altitude, and field length factor.

The study indicated that the minimum field length for the baseline study configuration was approximately 582 meters (1912 feet) for takeoff and 593 meters (1945 feet) for landing. The 60° flap setting, which made it possible to approach at 70 knots, best met the landing requirements. A decrease in flap deflection was necessary for a go-around maneuver with all engines operating. Results of a parametric study and an analysis of alternate flap settings indicated that the study configuration had considerable flexibility for purposes of meeting operational requirements and suggested several means of improving takeoff and landing performance.

INTRODUCTION

In recent years there has been considerable interest in short-takeoff-and-landing aircraft for both military and civil applications because of special performance requirements or field length restrictions. Civil applications for STOL aircraft could include short-haul air transportation. This could relieve the congestion in the present air transportation system and might provide quicker, more economical service than a ground transportation system for short and medium range markets. In military applications, STOL aircraft could permit rapid deployment and the use of short, unprepared landing areas for battlefield resupply.

Since a STOL airplane must operate safely from short fields (those approximately 610 m (2000 ft) long), taking off and landing must be feasible at speeds which are low (less than 100 knots) compared with those for conventional aircraft. Because of these low speeds, some type of propulsive lift system is necessary to augment the airplane's basic aerodynamic lift. One unproven but promising concept for turbofanjet-powered aircraft is an externally blown flap system. With this sytem, the exhaust flow from a conventional turbofan engine is directed onto the flaps so that the flow is diffused and deflected downward. Additional lift is generated as a result of the redirected thrust and by the supercirculation of airflow which occurs over most of the wing.

Considerable wind-tunnel research has been conducted on externally blown flap systems to determine their performance and stability and control characteristics (refs. 1 to 12). Recently, a program was undertaken at the NASA Flight Research Center to investigate the performance and stability and control characteristics of a jet STOL transport configuration that utilized the externally blown flap propulsive lift concept. This report presents the results of an analytical study which was made to assess the configuration's takeoff and landing performance and its field length requirements.

During this study, ground rules were defined for short-field takeoff and landing maneuvers, operational envelopes were determined, and takeoff and landing performance and field length requirements were calculated. A parametric study was also performed to determine the effect of variations in selected parameters on takeoff and landing field length requirements.

SYMBOLS

Physical quantities in this report are given in the International System of Units (SI) and parenthetically in U.S. Customary Units. Calculations were made in Customary Units. Factors relating the two systems are presented in reference 13.

a_n acceleration normal to flightpath, m/sec^2 (ft/sec^2)

C_L lift coefficient, $\frac{Lift}{qS}$

$\bar{c}$	wing mean aerodynamic chord, m (ft)
g	acceleration due to gravity, m/sec^2 (ft/sec^2)
h	altitude, m (ft)
q	free-stream dynamic pressure, N/m^2 (lbf/ft^2)
R/C	rate of climb
S	wing reference area, m^2 (ft^2)
T	thrust, N (lbf)
ΔT_a	change in ambient temperature from standard day value, °K (°F)
V	velocity, knots
V_{mc}	minimum control speed, knots
V_{min}	minimum speed, knots
V_s	stall speed, knots
V_1	critical decision speed, knots
V_2	speed at barrier height, knots
W	weight, kg (lbm)
α	angle of attack, deg
γ	flightpath angle, deg
δ_f	wing trailing-edge flap deflection (fig. 2)
θ	pitch attitude, deg

Subscripts:

app	approach condition
lof	lift-off condition
max	maximum
td	touchdown condition

All speeds are in knots equivalent airspeed.

JET STOL TRANSPORT CONFIGURATION

The jet STOL transport configuration used in this study is illustrated by the model shown in figure 1. The study configuration had a high wing, high T-tail, and four pod-mounted high-bypass-ratio turbofanjet engines located under and forward of the wings. The wing was equipped with leading-edge flaps and full-span, externally blown, triple-slotted trailing-edge flaps. The full-span trailing-edge flaps on each wing semispan were composed of three spanwise segments (fig. 2(a)). The engines were mounted so that the flow of the jet and fan exhaust impinged directly on the trailing-edge flaps when deflected (fig. 2(b)), thereby incorporating the externally blown flap propulsive lift concept.

The study configuration weighed 21,772 kilograms (48,000 pounds mass), had a sea-level standard day installed thrust of 30,025 newtons (6750 pounds force) per engine, and had a wing reference area of 55.7 square meters (600 square feet). This established a thrust-to-weight ratio of 5.516 N/kg (0.563 lbf/lbm) and a wing loading of 391 kg/m^2 (80 lbm/ft^2). The dimensions of this configuration, referred to herein as the baseline configuration, are shown in table 1. This baseline configuration could be representative of an experimental STOL transport research airplane.

For the study configuration, provisions for longitudinal control and trim requirements were made by using a movable horizontal stabilizer which could be deflected $\pm 10^\circ$. Incorporated in the horizontal stabilizer were elevator surfaces and leading-edge Krueger flaps which were geared to the horizontal stabilizer position. Unless otherwise noted, the aerodynamic characteristics used in this study were based on measured data from a 2.4-meter (8-foot) model which was tested in the Langley 30- by 60-foot full-scale wind tunnel as reported in reference 12. Unless noted otherwise, the data used were for a configuration with engines at the 0.22 and 0.42 wing semispan locations, herein called the spread-engine configuration. The wing leading-edge flaps were deflected 60° and the center of gravity was at the 40-percent mean aerodynamic chord in all cases. Jet exhaust deflectors were not used. The data that were selected excluded boundary-layer control effects on the wing leading edges, ailerons, and tail surfaces. Some extrapolation of the wind-tunnel data was necessary for low speed and high power conditions where the gross thrust coefficient exceeded the values used in the wind-tunnel tests.

The wind-tunnel data were modified by increasing the rudder control effectiveness to be representative of a double-hinged rudder design. The wind-tunnel data were based on a model configuration without a landing gear; a drag coefficient of 0.03 was added to simulate an extended tricycle type of landing gear. A maximum rotation angle of 15° was assumed to prevent tail scraping.

The turbofanjet performance characteristics are based on a TF34-GE-2 turbofan engine with a nominal bypass ratio of 6.0 (ref. 14). The engine has an uninstalled sea-level static thrust rating of 41,280 newtons (9280 pounds force); however, a significant reduction in noise can be achieved by operating at reduced power. For the baseline configuration of this study, the engine was throttled to provide an installed thrust level of 30,025 newtons (6750 pounds force) per engine for normal four-engine operation. Higher thrust levels were permitted for emergency conditions where noise constraints would not apply.

Takeoff Configuration

All takeoff performance calculations were made for a configuration in which the third (trailing-edge) flap element deflection angle was 35°. Takeoff performance calculations used the spread-engine configuration data; however, the operational envelope and takeoff reference speeds were determined from clustered-engine configuration data (engines placed at the 0.22 and 0.30 wing semispan locations) because of the more complete data base available in reference 12. It should not be assumed that a 35° flap setting is optimal for the takeoff maneuver: this was the only takeoff flap setting for which data were available in the reference 12 data base.

Landing Configuration

Spread-engine configuration characteristics from reference 12 were used to investigate the landing performance characteristics for flap deflection angles of 40°, 50°, and 60°. Data for the 50° flap setting were based on a linear interpolation between the measured data for the 40° and 60° flap settings.

Engine-Out Procedure

In this study the critical engine-out condition refers to the failure of an outboard engine. Engine-out procedures used were established in a fixed-base simulator study of this configuration which was performed at the Flight Research Center. The engine-out procedure involved the differential deflection of the third element of the center-span flaps to reduce the aileron deflection requirements. Full-span conventional spoilers were also used in conjunction with the ailerons when the ailerons were deflected more than 10°. This procedure was used for all flap settings; however, the differential flap deflection required varied from 13° for the 35° flap setting to 40° for the 60° flap setting. Engine-out characteristics for the configuration with the 50° flap setting are based on a linear interpolation between engine-out characteristics for configurations with the 40° and 60° flap settings.

The maximum sea-level static installed thrust permitted for the critical engine-out go-around and landing maneuvers where noise constraints were not in effect was 32,027 newtons (7200 pounds force) per engine. This thrust level would represent the design thrust-to-weight ratio of 5.52 N/kg (0.60 lbf/lbm) if all four engines were operating at maximum power.

METHOD OF ANALYSIS

Certain ground rules and procedures were defined and used to calculate short-field takeoff and landing maneuvers and to determine field length requirements. The existing civil airworthiness standards (refs. 15 and 16) are not directly applicable to powered-lift jet STOL transport aircraft. The Federal Aviation Administration (FAA) has published tentative airworthiness standards (ref. 17) which provide some guidelines concerning the certification requirements for takeoff and landing; however, flight experience with jet STOL aircraft will be necessary before these standards can be adopted as FAA regulations.

Takeoff

The takeoff ground rules cover three different takeoff maneuvers. They are based primarily on the guidelines in references 17 and 18. The three maneuvers are normal four-engine takeoff, critical engine-out continued takeoff, and rejected takeoff.

Normal four-engine takeoff. — A sketch of the normal four-engine takeoff maneuver is shown below.

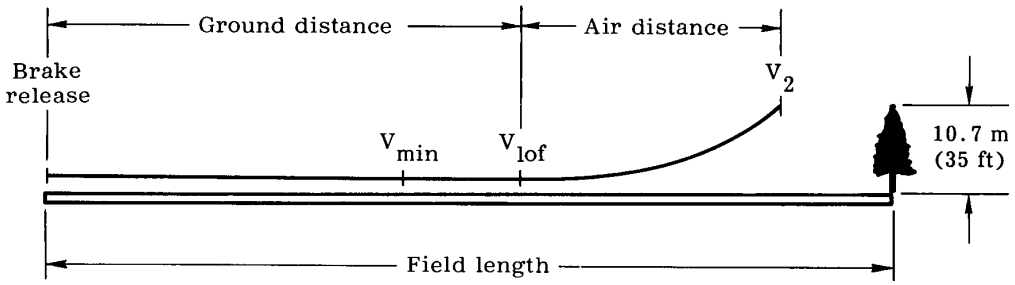

The normal four-engine takeoff ground rules are:

- Minimum speed, V_{min}, must not be less than V_{mc} or V_s with the critical engine out at takeoff power with pitch, yaw, and roll moments trimmed to zero.
- Lift-off speed, V_{lof}, must be greater than or equal to $1.05V_{min}$.
- Angle of attack at lift-off, α_{lof}, must be less than or equal to the aircraft's tail-scraping angle minus 3°.
- Rate of climb at lift-off, R/C_{lof}, must be greater than or equal to 1.27 meters per second (250 feet per minute) with the landing gear extended and the critical engine out at takeoff power.
- Speed at the barrier height, V_2, must not be less than $1.10V_{min}$ or V_{min} plus 15 knots.
- Rate of climb, R/C, must be greater than or equal to 1.52 meters per second (300 feet per minute) at V_2 with the landing gear retracted and the critical engine out at takeoff power.
- Field length is determined by adding a 15-percent margin to the takeoff distance.

The maneuver begins at brake release. The airplane accelerates to lift-off speed, V_{lof}, with four engines operating at maximum takeoff power. After lift-off, the airplane climbs to 10.7 meters (35 feet), the height of an assumed obstacle. The speed

of the airplane at this height is the reference speed, V_2. It was assumed that aircraft rotation was initiated 3 knots below V_{lof} for all calculations of takeoff performance.

Critical engine-out continued takeoff.— A sketch of the continued takeoff maneuver with the critical engine out is shown below.

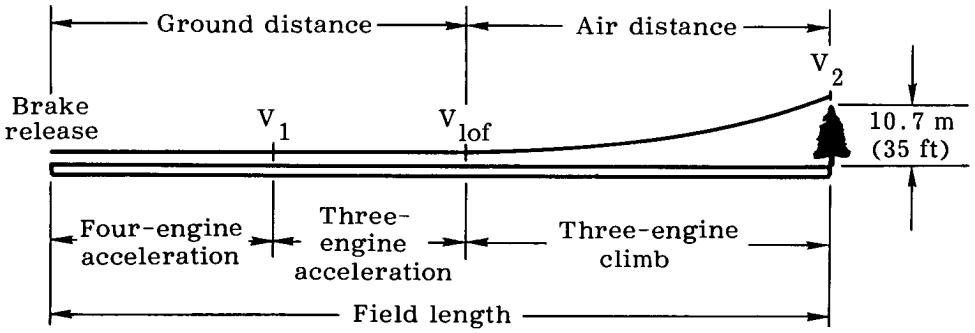

The critical engine-out continued takeoff ground rules are:

- The speed at which the decision is made to continue or reject the takeoff, V_1, must not be less than V_{min}.
- Lift-off speed, V_{lof}, and the speed at the barrier height, V_2, are the same as for normal four-engine takeoff.
- Field length is the critical engine-out continued takeoff distance.

In this maneuver the airplane accelerates using four engines at maximum takeoff power up to the critical decision speed, V_1, where an outboard engine is assumed to fail. The airplane then continues the takeoff with the critical engine out. The maneuver is complete when the airplane attains the 10.7-meter (35-foot) obstacle height. The speed V_1 also represents the velocity at which the distance required for the continued takeoff equals the distance required for the rejected takeoff.

Rejected takeoff.— A sketch of the rejected takeoff maneuver is shown below.

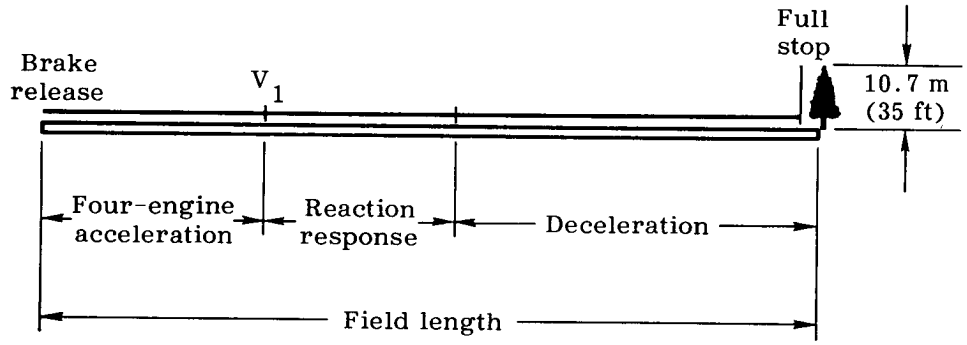

The rejected takeoff ground rules are:

- The speed at which the decision is made to continue or reject the takeoff, V_1, must not be less than V_{min}.
- Time required for pilot recognition, reaction, and response to emergency condition is 2 seconds.
- Average rollout deceleration rate is 0.4g.
- Field length is equal to the rejected takeoff distance.

For this maneuver the airplane accelerates on four engines at maximum takeoff power up to the critical decision speed, V_1, where a failure is assumed to occur and the takeoff maneuver is aborted. After reaching V_1, 2 seconds are allowed for recognition, reaction, and response, during which speed remains constant; then the airplane is braked to a safe stop at an assumed average deceleration rate of 0.4g.

In this study all takeoff performance calculations are based on a sea-level standard day condition with no wind or ground effects. A rolling friction coefficient of 0.025 was used. The field length required for takeoff is established by the larger of the field lengths determined for the (1) normal four-engine takeoff or (2) the continued and rejected takeoff maneuvers.

The steady-state performance characteristics used to develop an operational envelope were determined from aerodynamic characteristics which were functions of angle of attack, speed, altitude, and power setting. For the critical engine-out condition, roll and yaw trim requirements were included. Minimum control speeds and 1g stall speeds were defined, and takeoff reference speeds were established.

Approach and Landing

A sketch of the approach and landing maneuver is shown below.

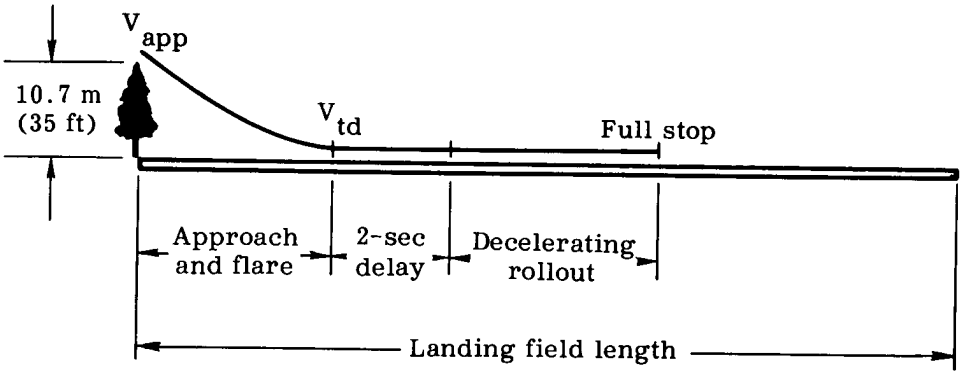

The approach and landing ground rules are:

- Minimum speed, V_{min}, must not be less than (1) V_{mc} or V_s for four-engine operation at the approach power setting or (2) V_{mc} or V_s for

the critical engine-out condition at maximum power.

- Approach speed, V_{app}, must not be less than V_{min} plus 10 knots or $1.15V_{min}$.
- Touchdown speed, V_{td}, must not be less than V_{min}.
- Nominal approach vertical descent rate is 4.06 meters per second (800 feet per minute).
- Maximum approach vertical descent rate is 5.08 meters per second (1000 feet per minute).
- Approach angle of attack, α_{app}, must be 10° less than stall angle of attack.
- Partial flare to a rate of descent of -0.91 meter per second (-3 feet per second) at touchdown is required.
- Delay between touchdown and start of deceleration is 2 seconds.
- Average rollout deceleration rate is 0.35g.
- The airplane must have the capability to continue the approach with the critical engine out.
- Go-around requires (1) a rate of climb of 1.27 meters per second (250 feet per minute) at V_{app}, using four engines at maximum power and (2) a rate of climb of 1.14 meters per second (225 feet per minute) at V_{app} plus 20 knots, using three engines at maximum power.
- Flap setting and power setting changes are allowed.
- Landing field length is determined by dividing the landing distance by a factor of 0.6.

The maneuver consists of an approach over a 10.7-meter (35-foot) obstacle at a constant rate of descent. There is a partial flare before touchdown. Touchdown is followed by a 2-second delay before deceleration. The maneuver is completed after deceleration to full stop.

According to the ground rules, no speed margin was required at touchdown; therefore, some of the speed margin provided by increasing V_{min} by 10 knots or 15 percent could be used to perform the partial flare.

Most of the go-around requirements used in this study are specified in reference 17. Two exceptions to these requirements were made in that changes in flap and power settings were allowed during the go-around maneuver.

The steady-state performance characteristics were used to determine minimum control speeds and 1g stall speeds for both four- and three-engine operation. The

specified speed margins were added, and the minimum safe approach speed was determined.

RESULTS AND DISCUSSION

Takeoff and landing performance calculations were made with a conventional two-dimensional, point mass, digital trajectory program. This program calculated the distances traveled, speeds, attitude angles, and other pertinent parameters from the aerodynamic and propulsion system characteristics and presented them in time history format. The distance traveled during the 2-second delay prior to braking and the decelerating rollout was determined by hand calculation.

Takeoff

Baseline performance. — Takeoff performance calculations were based on the baseline configuration with a flap setting of 35°. Figure 3 shows the operational envelope and takeoff reference speeds (that is, V_{min}, V_{lof}, and V_2) determined by using the ground rules and procedures described in the METHOD OF ANALYSIS section. The operational envelope, which is plotted in terms of flightpath angle as a function of airplane velocity, is limited at the top by the maximum power setting for four engines and at the bottom by the boundary of flight capability of four engines operating at 30-percent power. The boundary at the lower left is based on $C_{L_{max}}$ (the point at which 1g stall occurs) for four engines operating at power settings from 30 percent to 100 percent. The intermediate line shows the limit of flight capability of three engines operating at maximum power with all pitch, roll, and yaw moments trimmed to zero and with zero bank and sideslip angle.

The minimum speed, V_{min} (point A), was determined to be 65.5 knots because of the aileron deflection limit of 60° for three-engine operation. A 5-percent speed margin was added to this minimum speed, defining a minimum lift-off speed of 69 knots (point B). However, the requirement for a rate of climb of at least 1.27 meters per second (250 feet per minute) at lift-off with the critical engine out raised the lift-off speed to approximately 78.5 knots (point C). At the 10.7-meter (35-foot) obstacle, V_2 was determined to be 80.5 knots (point D) because of the ground rule that added 15 knots to V_{min}. This speed easily meets the only other requirement for V_2, that is, that it allow a minimum rate of climb of 1.52 meters per second (300 feet per minute) with the critical engine out and the landing gear retracted. Figure 3 also shows climbout to be possible at an angle greater than 10° at V_2 with four engines operating at maximum power.

The takeoff performance of the baseline configuration is shown in figures 4(a), 4(b), and 4(c). In figure 4(a) the airplane used 310 meters (1016 feet) to accelerate from brake release to lift-off velocity and 138 meters (454 feet) to climb from lift-off to 10.7 meters (35 feet). Therefore the normal four-engine takeoff distance was 448 meters (1470 feet), and the field length was 515 meters (1691 feet). The

airplane accelerated to a speed of 87 knots at the 10.7-meter (35-foot) obstacle height, exceeding the requirement for V_2.

Figures 4(b) and 4(c) show the critical engine-out continued takeoff and the rejected or aborted takeoff, respectively. In both maneuvers the airplane accelerated from brake release to the critical decision point, which for this study was defined as the velocity at which rotation occurred. At the critical decision point, an outboard engine failure occurred and the takeoff continued with three engines. For the critical engine-out maneuver, an additional 62 meters (206 feet) were used to accelerate to lift-off speed, and 239 meters (783 feet) were used to climb to 10.7 meters (35 feet). The airspeed at that height was 85 knots, meeting the V_2 requirement. For the rejected takeoff operation, after reaching the speed where the engine was assumed to have failed, 2 seconds were allowed for failure recognition and corrective action. Corrective action consisted of reducing the thrust of the remaining engines and applying the brakes. During the reaction and response time, 83 meters (272 feet) were traveled. The deceleration portion of the operation, at an average deceleration rate of 0.4g, covered a distance of 218 meters (717 feet). Therefore, for both of these operations the distance used and the field length required was 582 meters (1912 feet).

Time histories for the normal four-engine takeoff and the three-engine continued takeoff are shown in figure 5. For the four-engine takeoff, the airplane took approximately 12 seconds to reach the lift-off speed of 83.5 knots. The angle of attack required for lift-off at that velocity was 3.4°. After lift-off the aircraft rotated to a pitch attitude of 14.7° and flew at that attitude to an altitude of 10.7 meters (35 feet). From brake release to obstacle height, this maneuver required a total elapsed time of approximately 16 seconds. For the critical engine-out continued takeoff, V_1 occurred at the point of vehicle rotation. The angle of attack required to lift off was 5.6°. This greater angle of attack, combined with a reduced rate of acceleration after the engine failed, caused the continued takeoff distance to exceed the normal four-engine takeoff distance by 134 meters (440 feet). The increase in time due to an engine failure for the airplane to reach 10.7 meters (35 feet) was determined to be approximately 3 seconds.

Parametric study.— Calculations were also performed to assess the effects of variations in selected parameters on takeoff field length requirements.

Figure 6 shows the effect of wing loading on takeoff field length requirements. Thrust and weight were kept at the baseline values while the wing area was varied to cover a range from 341.8 to 439.4 kg/m^2 (70 to 90 lbm/ft^2). The increase in field length due to increasing W/S was nearly linear over the range studied. Increasing W/S by 48.8 kg/m^2 (10 lbm/ft^2) caused an average increase in field length of 38 meters (125 feet) for the four-engine takeoff and 49 meters (160 feet) for the three-engine continued takeoff.

The effect of thrust-to-weight ratio on takeoff field length is shown in figure 7. For this study, weight was kept at the baseline value and thrust was varied to cover a range from 4.9 to 6.1 N/kg (0.50 to 0.625 lbf/lbm). An increase in T/W of approximately 10 percent from the baseline value decreased the takeoff field length

by approximately 18 percent (93 meters (305 feet)). For a takeoff field length of 610 meters (2000 feet) or less, T/W must be greater than 5.5 N/kg (0.56 lbf/lbm) based on the three-engine continued takeoff.

Figure 8 shows the change in field length as a function of weight. For these calculations the thrust and wing reference area were kept at the baseline values as weight was varied. For the three-engine continued takeoff maneuver, a 10-percent increase in weight from the baseline value increased the takeoff field length by 33 percent (193 m (630 ft)). A 10-percent decrease in weight decreased the takeoff field length by 23 percent (137 m (450 ft)).

The effects of ambient temperature and elevation on takeoff field length are shown in figures 9(a) and 9(b). Figure 9(a) shows that an 11° K (20° F) decrease in temperature from the standard day value decreased the takeoff field length by 76 meters (250 feet), whereas a 16° K (30° F) increase in temperature increased the takeoff field length by 2.87 meters (940 feet). Figure 9(b) shows that the takeoff field length is 88 meters (290 feet) longer at an elevation of 610 meters (2000 feet) than it is at sea level.

The effects of deceleration rate and reaction-response time on takeoff field length for the rejected takeoff maneuver are shown in figure 10. The field length for the rejected takeoff maneuver would be reduced by 73 meters (240 feet) if the average deceleration rate were 0.6g during rollout instead of 0.4g, the baseline value. The reaction-response time after engine failure and before braking started had a linear effect on field length for the rejected takeoff. A 2-second variation in the delay time changed the field length required for the rejected takeoff maneuver by 82 meters (270 feet).

Landing

Baseline performance.— Landing performance calculations were based on the baseline configuration with flap settings of 40°, 50°, and 60°.

Flap setting of 60°: The ground rules and procedures described in the METHOD OF ANALYSIS section were used to develop the operational envelope shown in figure 11, which is for a flap setting of 60°. The operational envelope is limited at the top by the maximum power setting with four engines operating. The limit of flight capability for four engines operating at 30-percent power is shown by the line at the lower right. The boundary at the lower left is based on the $C_{L_{max}}$ limits for four-engine operation over the power setting range from 30 percent to 100 percent. The flight capability at maximum power with three engines operating is shown by the intermediate line. The requirement for continuing the approach with a critical engine out prohibited the use of that portion of the envelope above the line indicating maximum three-engine power. The dashed lines indicate a 1.27-meter-per-second (250-foot-per-minute) climb capability, the desired 4.06-meter-per-second (800-foot-per-minute) approach descent rate, and a maximum rate of descent at low altitude of 5.08 meters per second (1000 feet per minute).

The minimum speeds are defined by the $C_{L_{max}}$ boundary. Adding the 10-knot or 15-percent speed margin to the minimum speed along the line of constant power setting defines the minimum approach speeds. The shaded area in the figure represents the speed margin for a range of approach power settings with all engines operating and is bounded on the left by the line indicating maximum three-engine power. The approach speed of interest is defined by the intersection of the line for the minimum approach speed and the line for the 4.06-meter-per-second (800-foot-per-minute) rate of descent. Thus V_{app} for the 60° flap setting was determined to be 70 knots (point B) and would require a power setting of 68 percent. The corresponding minimum speed for four-engine operation at a power setting of 68 percent is 60 knots (point A). The V_{min} speed of 57.5 knots (point C) and V_{app} speed of 70 knots (point B) for three-engine operation at maximum power does not place any additional constraint on approach performance.

Figure 11 also shows that the ground rules for the go-around maneuver with four engines operating require an acceleration to higher speed or a decrease in flap setting or some combination of the two. To perform a go-around maneuver with an engine out, both an increase in speed and a decrease in flap setting are required.

The landing performance of the baseline configuration with a flap setting of 60° is shown in figure 12 for an approach at 70 knots. The approach was made over a 10.7-meter (35-foot) obstacle, and a partial flare maneuver was performed to achieve a vertical descent rate of 0.9 meter per second (3 feet per second) at touchdown. The partial flare maneuver was accomplished by increasing the angle of attack; other techniques were considered to be beyond the scope of this study. The actual landing distance was calculated to be 356 meters (1168 feet), which defined a landing field length for the baseline configuration of 593 meters (1945 feet).

A time history of the landing maneuver is shown in figure 13. The top plot shows the variation of distance with time, and the center plot shows the variation of altitude and speed with time. Touchdown occurred at a speed of 65 knots, so 5 knots were bled off during the partial flare maneuver. A 5-knot speed margin existed at touchdown. The variation of angle of attack, pitch attitude, and flightpath angle with time is shown in the bottom plot in figure 13. The flightpath angle at touchdown was -1.6°. Touchdown angle of attack was 14.2°, close to the assumed tail-scraping angle of 15°.

Alternate flap settings: Operational envelopes and performance characteristics were also investigated for the 50° and 40° flap settings for the baseline configuration. The operational envelope for 50° flaps is shown in figure 14. As in figure 11, the low speed boundary and V_{min} speeds are defined by the $C_{L_{max}}$ limits. After the speed margin boundary was placed, the speed at which an approach could be made at a 4.06-meter-per-second (800-foot-per-minute) rate of descent was determined to be 84 knots (point B). The four-engine power setting for this speed is 43 percent. For this power setting V_{min} is 73 knots (point A). The landing field length for this approach speed was calculated to be 792 meters (2600 feet). It is possible to approach at speeds as low as 76 knots (point D) with this flap setting; however, a decrease in flightpath angle during the approach is required, and the landing field length requirements remain the same. Go-around was possible at all of the acceptable approach speeds, but only with four engines operating.

The operational envelope for a 40° flap setting is shown in figure 15. Again, the low speed boundary and V_{min} speeds are defined by the $C_{L_{max}}$ limits. The minimum approach speed for a 4.06-meter-per-second (800-foot-per-minute) rate of descent for this flap setting was determined to be 99 knots (point B). The four-engine power setting for this speed is 38 percent. For this power setting V_{min} is 84 knots (point A). The landing field length for this approach speed was calculated to be 1042 meters (3420 feet). It is possible to approach at speeds as low as 77 knots with this flap setting, but since a change in flightpath angle during the approach is required, landing field length requirements remain the same. Go-around was possible at all of the acceptable approach speeds, but only with four engines operating.

The variation of approach characteristics and landing performance for the previously discussed flap settings of 40° to 60° is shown in figure 16. The variation of landing field length, approach C_L, and flightpath angle with flap setting is shown at the top of the figure. A flap setting of at least 59° is necessary to land on a 610-meter (2000-foot) runway using the ground rules and procedures adopted for this study. The variation of angle of attack and power setting with flap deflection is shown by the plots in the center of the figure. The variation of V_{app} and V_{min} with flap setting is shown at the bottom of the figure.

Descent characteristics: A comparison of the descent characteristics for an approach velocity rate of 50 knots to 100 knots is shown in figure 17 for flap settings of 40°, 50°, and 60°. These characteristics are based on four-engine operation. They are constrained only by a 1g stall speed at $C_{L_{max}}$ and do not make any allowance for speed, maneuver, or angle-of-attack margins. The variation of landing field length, approach C_L, and flightpath angle with approach velocity is shown at the top of the figure and is representative of all three approach flap settings investigated.

The percentage of power required for steady-state approach at a 4.06-meter-per-second (800-foot-per-minute) descent rate is shown in the center plot in figure 17. It is desirable to perform the approach with four engines operating at less than 75-percent power so that the approach can be continued with one engine out. The highest power requirement is for the 60° flap setting, which used 68-percent power at 70 knots. More power is necessary to approach at lower speeds for all the flap settings. The 60° flap setting required a higher power setting than the other flap settings throughout the approach speed range for approach speeds greater than 65 knots.

Figure 17 also shows that as approach speeds and flap settings decrease, approach angle of attack increases. Therefore many approach conditions occur at such a large angle of attack that the assumed 15° tail clearance angle is exceeded. Thus it would not be possible to use angle of attack alone to perform the partial flare maneuver at the lower approach speeds and flap settings.

Operational margins: The margins required for the safe operation of jet STOL aircraft during approach and landing have not yet been defined. No attempt is made to establish these safety margins in this study; however, some of the margins for the

4.06-meter-per-second (800-foot-per-minute) vertical descent rate and the three landing flap settings investigated are compared in figures 18, 19, and 20.

In this study a speed margin of 10 knots or 15 percent, whichever was larger, was applied to V_{min}. In figures 18, 19, and 20, V_{min} is the 1g stall speed at $C_{L_{max}}$. Figure 18(a) shows the variation in speed margin with approach velocity for four-engine operation when the throttles are advanced to full power; figure 18(b) shows the speed margin based on the approach power setting. In the 70- to 90-knot speed range at approach power settings, the speed margin for the 60° flap setting is 11 percent to 19 percent greater than it is for the 50° flap setting.

The maneuver margins available for each approach flap setting investigated when approaching at a vertical descent rate of 4.06 meters per second (800 feet per minute) are shown in figures 19(a) and 19(b) for the maximum power setting and the approach power setting, respectively. In the 70- to 90-knot speed range at approach power settings, the maneuver margin provided by the 60° flap setting is 13 percent to 17 percent larger than that provided by the 50° flap setting.

Figures 20(a) and 20(b) compare the angle-of-attack margins for the approach and maximum power settings for the three approach flap settings investigated. For both the approach and maximum power settings, the 60° flap setting provides a margin that averages 7° greater than that provided by the 50° flap setting in the 70- to 90-knot speed range. One of the ground rules specified in the METHOD OF ANALYSIS section for approach and landing called for a margin of at least 10° between the approach angle of attack and the stall angle of attack at the approach power setting. With this margin included, the minimum approach speeds were 62.5 knots for the 60° flap setting, 88 knots for the 50° flap setting, and 98 knots for the 40° flap setting. This requirement for a 10° angle-of-attack margin did not establish the approach speed used in this study for the baseline configuration. The 60° flap setting provides an angle-of-attack margin of 13° at a 70-knot approach speed.

Parametric study.— Calculations were performed to assess the effect of the variation of selected parameters on landing field length for the 60° flap setting.

Figure 21 shows that a weight increase of 10 percent above the baseline value increases the landing field length by 17.5 percent, whereas a weight reduction of 10 percent causes the landing field length to decrease by only 5 percent.

The effect of varying wing loading on landing field length is shown in figure 22(a). Thrust and weight were kept constant while wing reference area was varied to cover a range of W/S values from 292.9 to 439.4 kg/m^2 (60 to 90 lbm/ft^2). An increase in W/S of 48.8 kg/m^2 (10 lbm/ft^2) caused landing field length to increase 67 meters (220 feet).

Figure 22(b) shows the effect of varying T/W on landing field length. It is apparent that at T/W ratios less than the baseline value, which is 5.5 N/kg (0.56 lbf/lbm), there is insufficient thrust to continue a 70-knot approach with a critical engine out; thus approaches at higher speeds and longer landing fields

are necessary. For T/W ratios greater than the baseline value, V_{min} at the level of thrust required for approach does not change; thus, there is no improvement in landing performance.

The effects on landing field length of variations in the delay before braking, rollout deceleration rate, and field length factor are shown for an approach speed of 70 knots in figures 23(a), 23(b), and 23(c), respectively. The delay after touchdown and before braking begins had a linear effect on landing field length. As shown in figure 23(a), a 2-second variation in delay time changed the landing field length by 112 meters (367 feet). Figure 23(b) shows that increasing the average deceleration rate during rollout from 0.35g to 0.45g reduced the landing field length by 56 meters (185 feet). Figure 23(c) shows that increasing the field length factor from the baseline value of 0.60 to 0.75 reduced the landing field length by 117 meters (385 feet). Thus each of these parameters had a significant effect on the landing field length requirements. It should be realized that these parameters could be defined only tentatively at this time and that they may undergo considerable change as operational experience with jet STOL aircraft is acquired.

The effects on landing field length of variations in ambient temperature and altitude are shown in figures 24(a) and 24(b). Figure 24(a) shows that a reduction in ambient temperature below the standard day value did not change landing field length, for the same reason that an increase in T/W did not. For temperatures greater than standard day, approach speeds had to be increased to make it possible to continue a 4.06-meter-per-second (800-foot-per-minute) rate of descent with the critical engine out. A 16° K (30° F) increase in temperature from the standard day value increased the landing field length by 140 meters (460 feet). Figure 24(b) shows that for each 305-meter (1000-foot) increase in landing field elevation, an additional 30.5 meters (100 feet) was required for landing field length.

Flight flexibility.— The areas of normal operation in the operational envelopes shown in this report are rather restricted. It should be realized that these areas represent only the regions used for performance calculations, and that excursions can safely be made into the areas considered to be margins.

It should also be realized that the operational envelope can be shifted by both the airplane designer and the pilot to meet specific flight requirements. Some of the design and operational factors and their general effects on the position of the operational envelope are shown in figure 25. A variation in thrust or drag moves the envelope almost vertically, as shown. Variations in W/S tend to move the envelope horizontally. Changes in weight move the envelope diagonally, since this represents a variation in both T/W and W/S. Flap actuation also moves the envelope diagonally, so considerable flexibility exists for high and low speed approaches and go-around maneuvers because of the ability to select an optimum flap setting. It is important to understand and take full advantage of this flexibility in designing and developing a practical jet STOL transport.

CONCLUSIONS

An analytical study of the takeoff and landing performance of a jet STOL transport configuration with full-span, externally blown, triple-slotted flaps showed that:

1. The field length for the baseline configuration was determined by the approach and landing maneuver.

2. For an approach speed of 70 knots, the landing field length for the baseline configuration was 593 meters (1945 feet).

3. The minimum takeoff field length for the baseline configuration was 582 meters (1912 feet).

4. Of the flap settings investigated, the 60° setting best met the landing requirements. A decrease in flap setting or an increase in speed was required for go-around with four engines operating.

5. Operating the baseline configuration at elevations greater than 610 meters (2000 feet) above sea level or on days when the ambient temperature was more than 8.3° K (15° F) hotter than the standard day value required takeoff and landing fields more than 610 meters (2000 feet) long.

6. Parametric study results indicated that the operational envelope was flexible and could easily be shifted to meet specific flight requirements.

Flight Research Center,
National Aeronautics and Space Administration,
Edwards, Calif., July 27, 1973.

REFERENCES

1. Campbell, John P.; and Johnson, Joseph L., Jr.: Wind-Tunnel Investigation of an External-Flow Jet-Augmented Slotted Flap Suitable for Application to Airplanes With Pod-Mounted Jet Engines. NACA TN 3898, 1956.

2. Johnson, Joseph L., Jr.: Wind-Tunnel Investigation of the Static Longitudinal Stability and Trim Characteristics of a Sweptback-Wing Jet-Transport Model Equipped With an External-Flow Jet-Augmented Flap. NACA TN 4177, 1958.

3. Johnson, Joseph L., Jr.: Wind-Tunnel Investigation at Low Speeds of Flight Characteristics of a Sweptback-Wing Jet-Transport Airplane Model Equipped With an External-Flow Jet-Augmented Slotted Flap. NACA TN 4255, 1958.

4. Johnson, Joseph L., Jr.: Wind-Tunnel Investigation of a Small-Scale Sweptback-Wing Jet-Transport Model Equipped With an External-Flow Jet-Augmented Double Slotted Flap. NASA MEMO 3-8-59L, 1959.

5. Parlett, Lysle P.; Fink, Marvin P.; and Freeman, Delma C., Jr.: Wind-Tunnel Investigation of a Large Jet Transport Model Equipped With an External-Flow Jet Flap. NASA TN D-4928, 1968.

6. Parlett, Lysle P.; and Shivers, James P.: Wind-Tunnel Investigation of an STOL Aircraft Configuration Equipped With an External-Flow Jet Flap. NASA TN D-5364, 1969.

7. Freeman, Delma C., Jr.; Grafton, Sue B.; and D'Amato, Richard: Static and Dynamic Stability Derivatives of a Model of a Jet Transport Equipped With External-Flow Jet-Augmented Flaps. NASA TN D-5408, 1969.

8. Parlett, Lysle P.; Freeman, Delma C., Jr.; and Smith, Charles C., Jr.: Wind-Tunnel Investigation of a Jet Transport Airplane Configuration With High Thrust-Weight Ratio and an External-Flow Jet Flap. NASA TN D-6058, 1970.

9. Freeman, Delma C., Jr.; Parlett, Lysle P.; and Henderson, Robert L.: Wind-Tunnel Investigation of a Jet Transport Airplane Configuration With an External-Flow Jet Flap and Inboard Pod-Mounted Engines. NASA TN D-7004, 1970.

10. Vogler, Raymond D.: Wind-Tunnel Investigation of a Four-Engine Externally Blowing Jet-Flap STOL Airplane Model. NASA TN D-7034, 1970.

11. Smith, Charles C., Jr.: Effect of Engine Position and High-Lift Devices on Aerodynamic Characteristics of an External-Flow Jet-Flap STOL Model. NASA TN D-6222, 1971.

12. Parlett, Lysle P.; Greer, H. Douglas; Henderson, Robert L,; and Carter, C. Robert: Wind-Tunnel Investigation of an External-Flow Jet-Flap Transport Configuration Having Full-Span Triple-Slotted Flaps. NASA TN D-6391, 1971.

13. Mechtly, E. A.: The International System of Units — Physical Constants and Conversion Factors (Revised). NASA SP-7012, 1969.

14. Anon.: TF34-GE-2 Turbofan Engine. Model Specification E1130. General Electric Co., Feb. 28, 1968.

15. Anon.: Federal Aviation Regulations. Part 25 — Airworthiness Standards: Transport Category Airplanes. FAA, Oct. 6, 1967.

16. Anon.: Federal Aviation Regulations. Part 121 — Certification and Operations: Air Carriers and Commercial Operators of Large Aircraft. FAA, Apr. 1, 1965.

17. Anon.: Tentative Airworthiness Standards for Powered Lift Transport Category Aircraft. Part XX. FAA, Aug. 1970.

18. Innis, Robert C.; Holzhauser, Curt A.; and Quigley, Hervey C.: Airworthiness Considerations for STOL Aircraft. NASA TN D-5594, 1970.

TABLE 1. — PHYSICAL CHARACTERISTICS OF THE BASELINE CONFIGURATION

Wing —	
Area, m^2 (ft^2)	55.7 (600)
Span, m (ft)	20.1 (66)
Aspect ratio	7.26
Length of mean aerodynamic chord, m (ft)	2.99 (9.8)
Sweep of quarter-chord line, deg	27.5
Vertical tail —	
Area, m^2 (ft^2)	11.1 (119)
Volume coefficient	0.09
Span, m (ft)	4.3 (14)
Horizontal tail —	
Area, m^2 (ft^2)	19.0 (205)
Volume coefficient	1.0
Span, m (ft)	10.1 (33)
Engines —	
Inboard location, percent wing semispan	22
Outboard location, percent wing semispan	42
Airplane —	
Weight, kg (lbm)	21,772 (48,000)
Wing loading, kg/m^2 (lbm/ft^2)	391 (80)
Thrust per engine (sea-level, static, standard day, installed), N (lbf)	30,025 (6750)
Thrust-to-weight ratio, N/kg (lbf/lbm)	5.516 (0.563)
Fuselage length, m (ft)	20.1 (66)

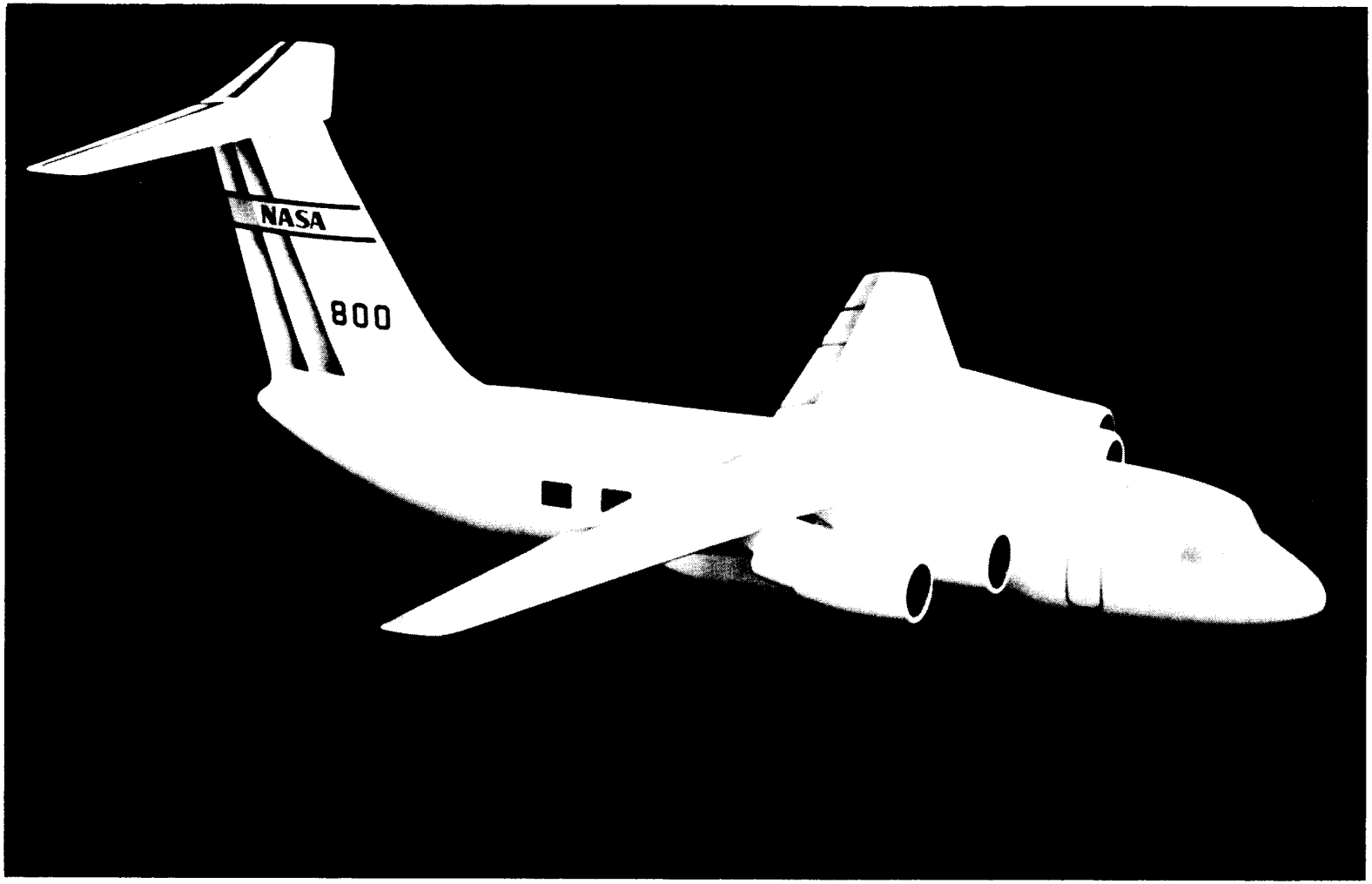

Figure 1. Experimental jet STOL transport configuration.

E-22755

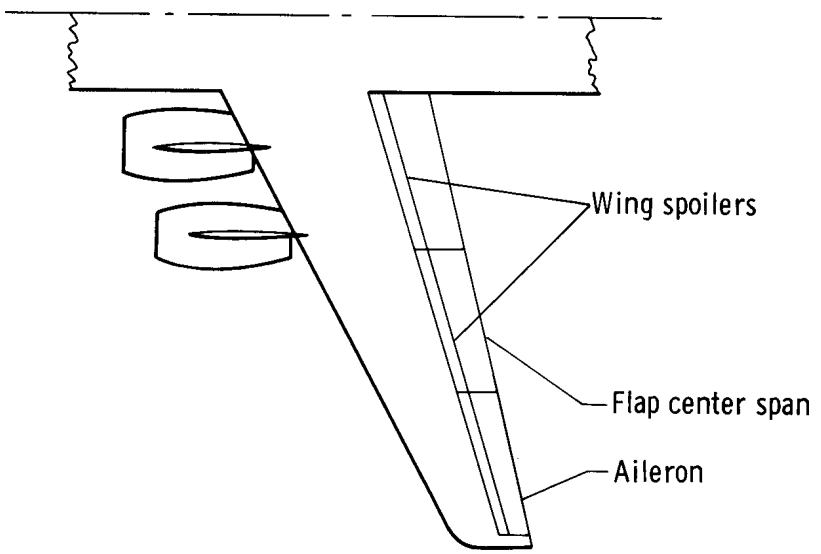

(a) Wing semispan.

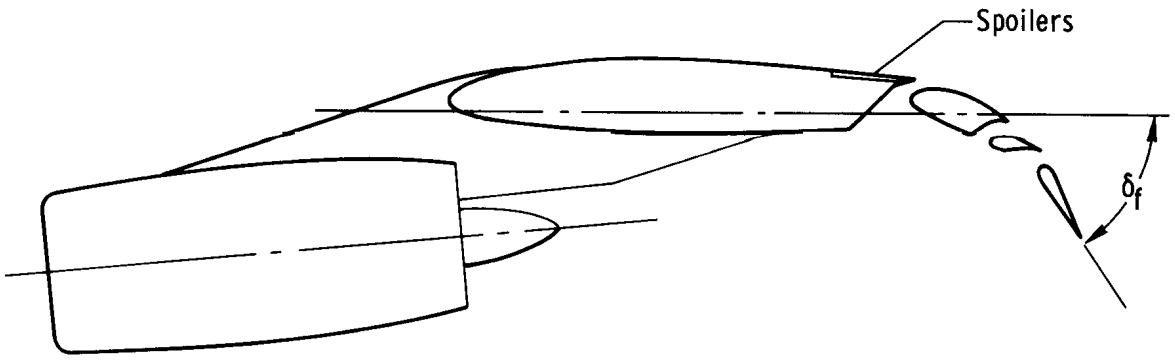

(b) Engine-pylon and wing-flap assembly.

Figure 2. Conceptual sketches of the study wing-flap-engine configuration.

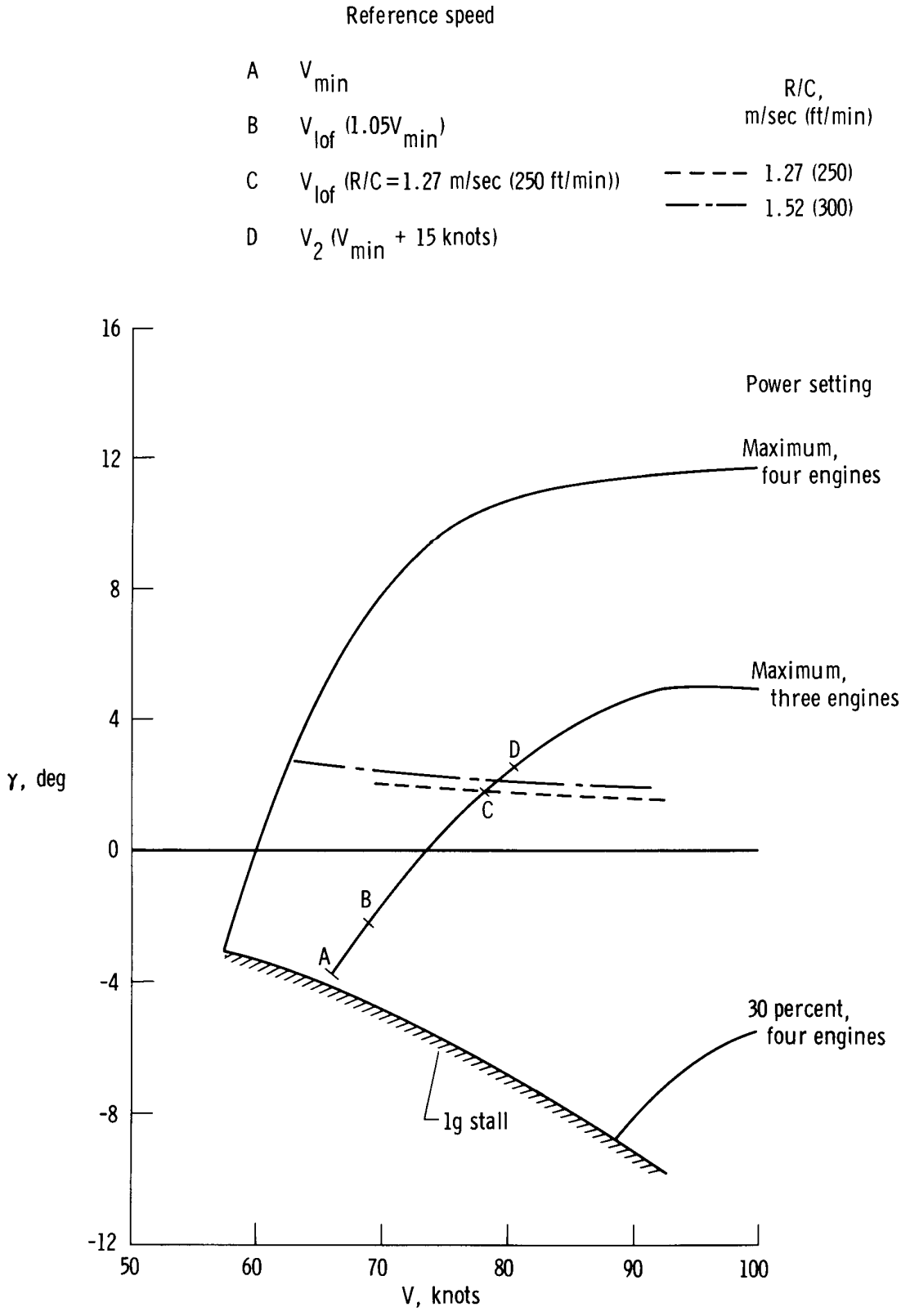

Figure 3. Operational envelope for takeoff. Baseline configuration; 35° flaps.

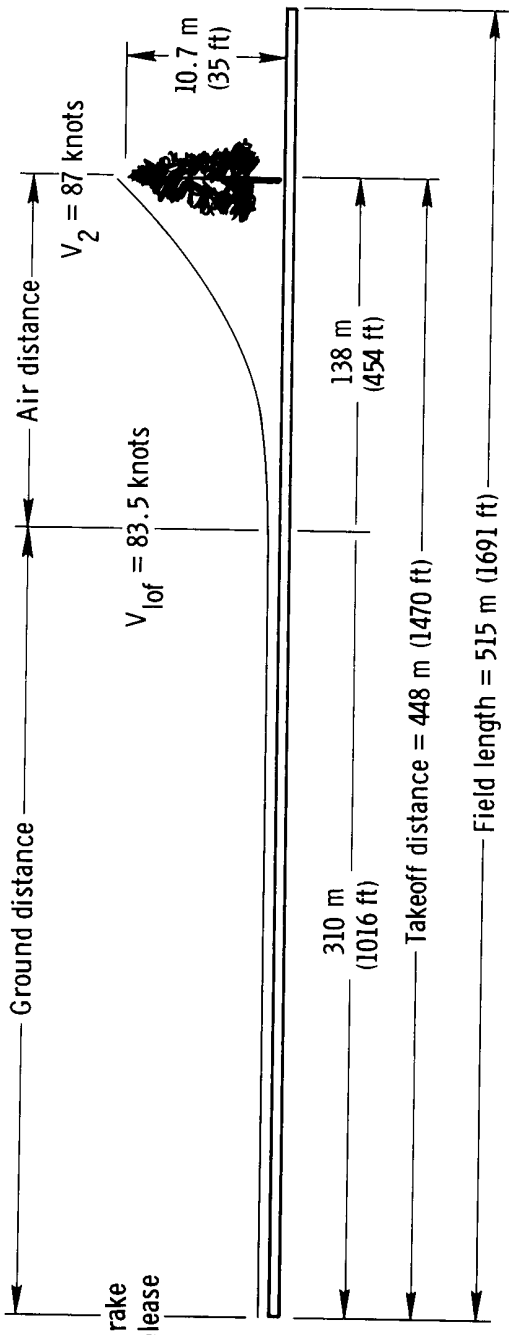

(a) Four-engine operation.

Figure 4. Takeoff performance. Baseline configuration; 35° flaps.

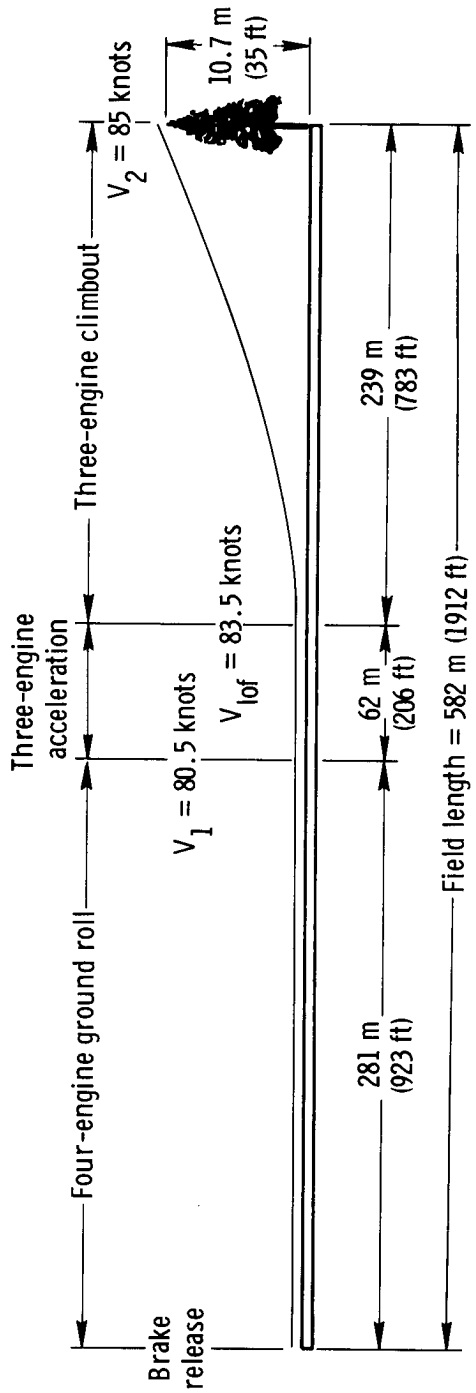

(b) Three-engine continued takeoff.

Figure 4. Continued.

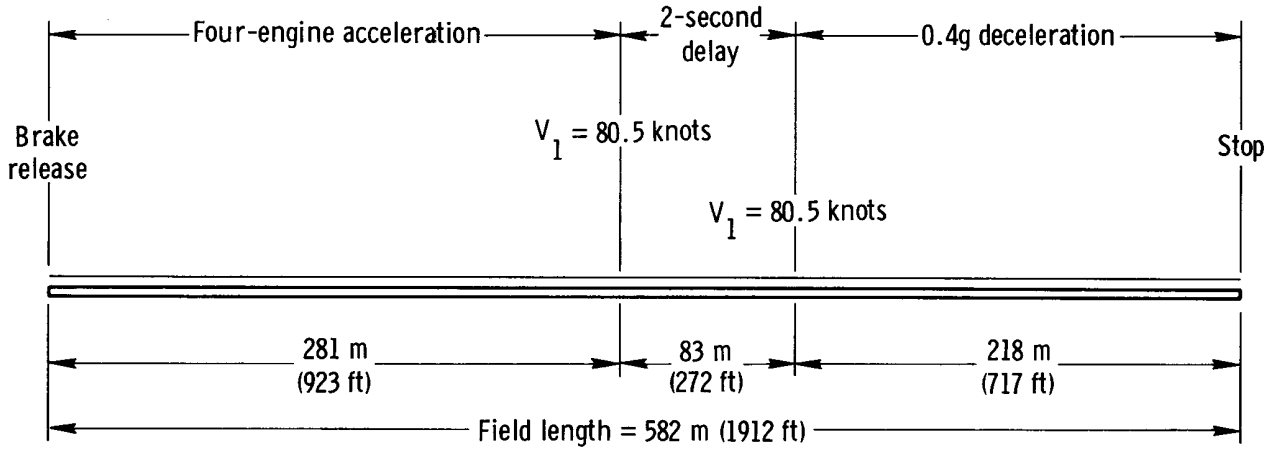

(c) Rejected takeoff.

Figure 4. Concluded.

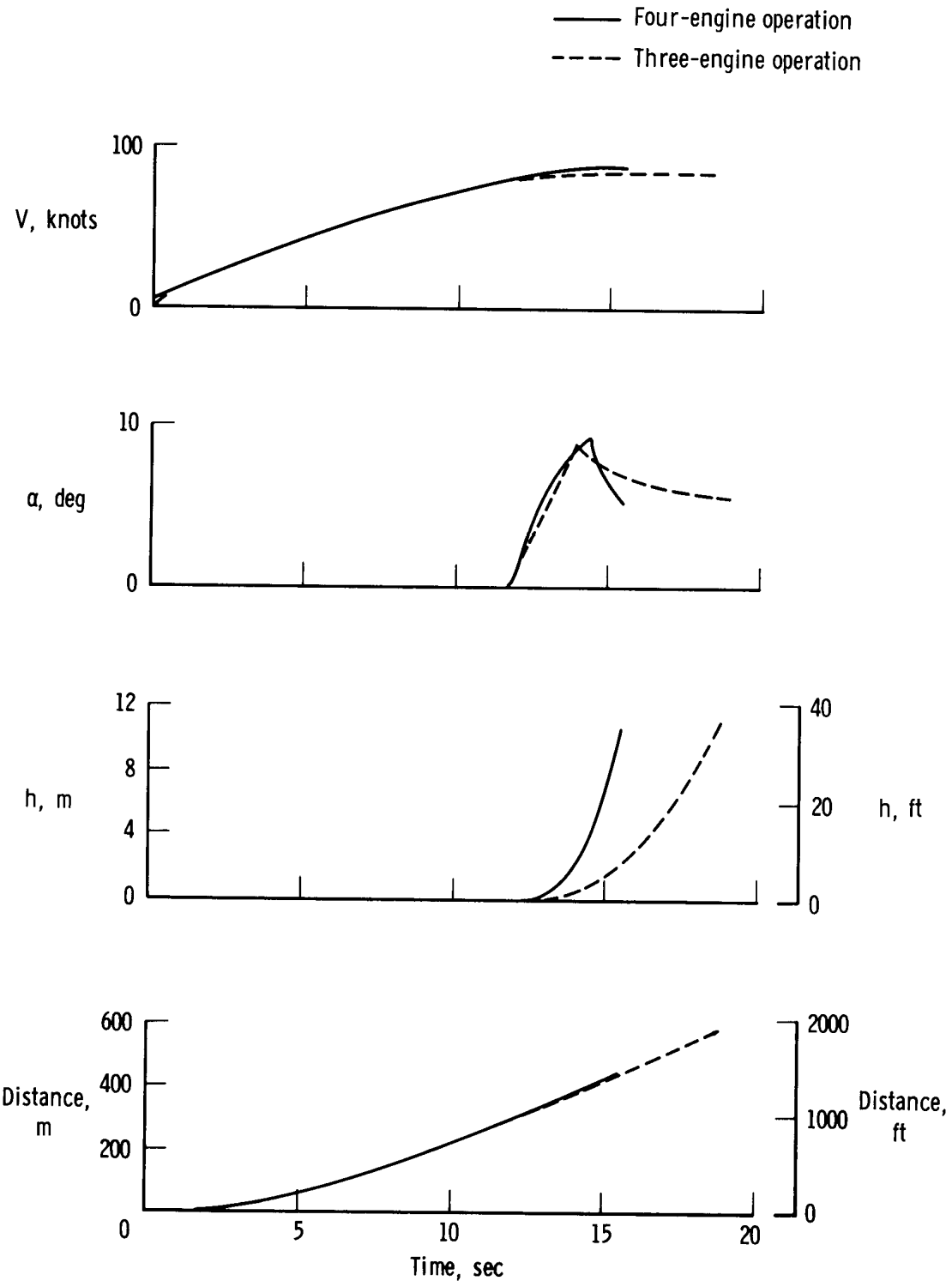

Figure 5. Time history of four-engine takeoff and three-engine continued takeoff. Baseline configuration; 35° flaps.

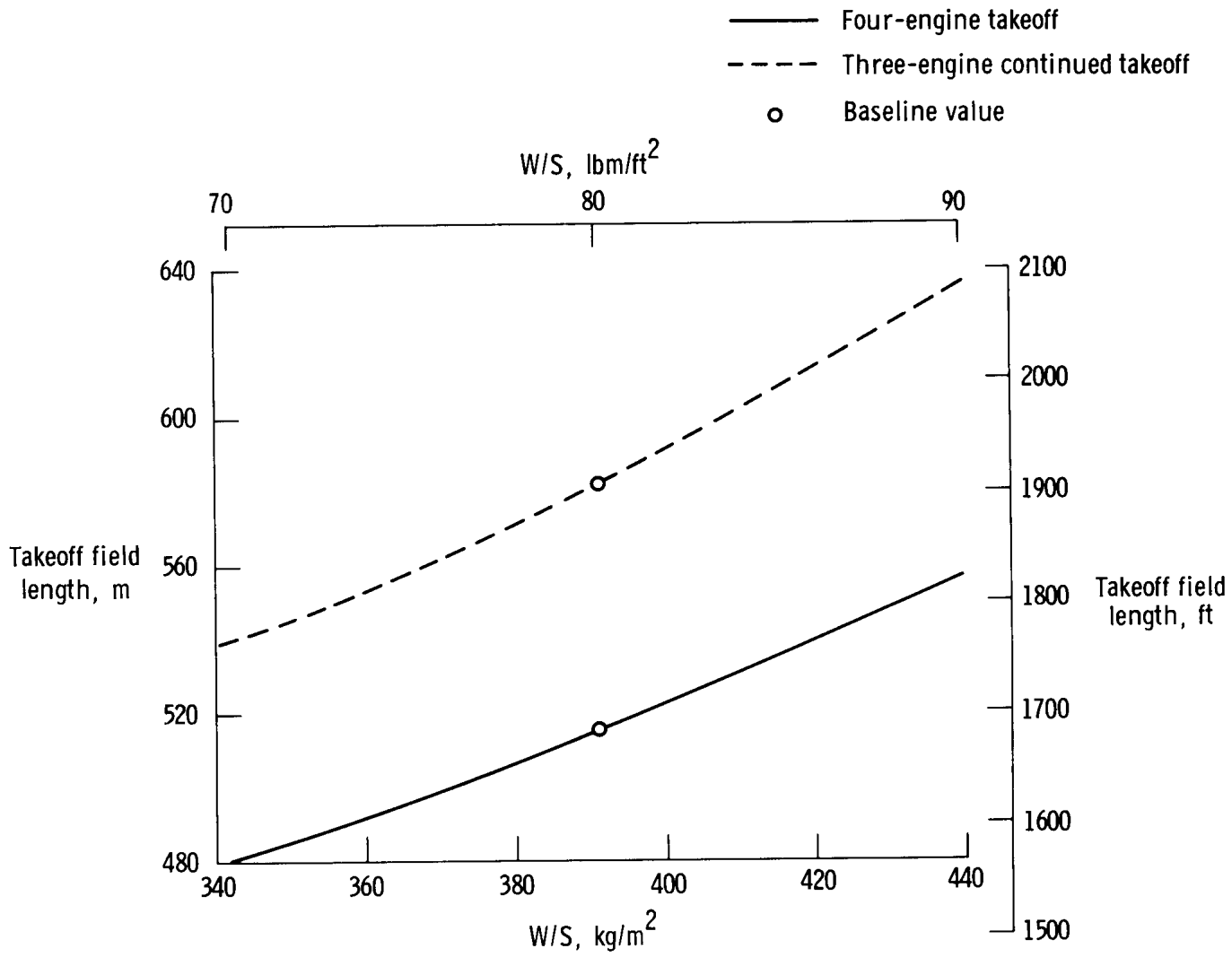

Figure 6. Effect of wing loading on takeoff field length. 35° flaps.

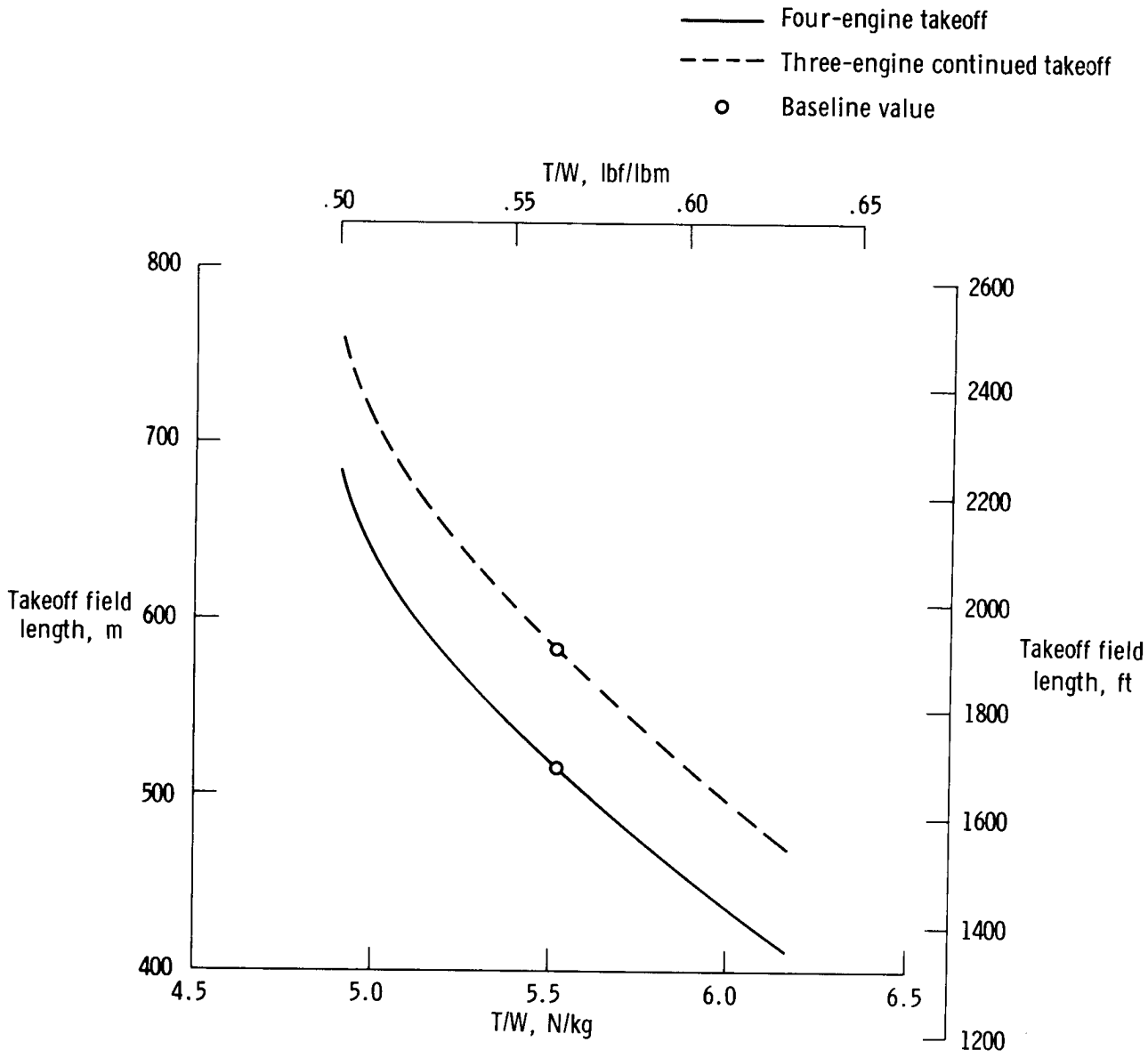

Figure 7. Effect of thrust-to-weight ratio on takeoff field length. 35° flaps.

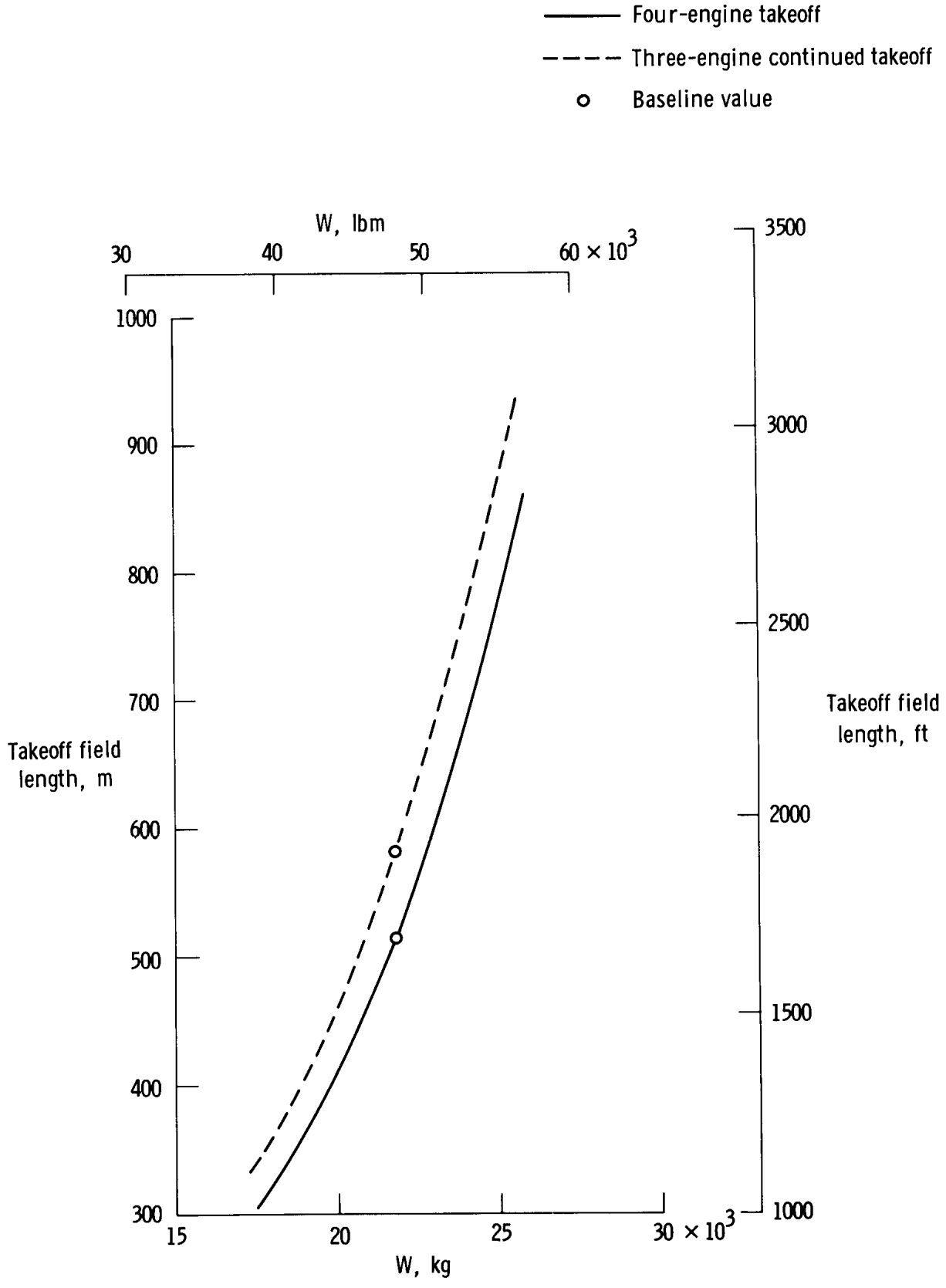

Figure 8. Effect of weight on takeoff field length. 35° flaps.

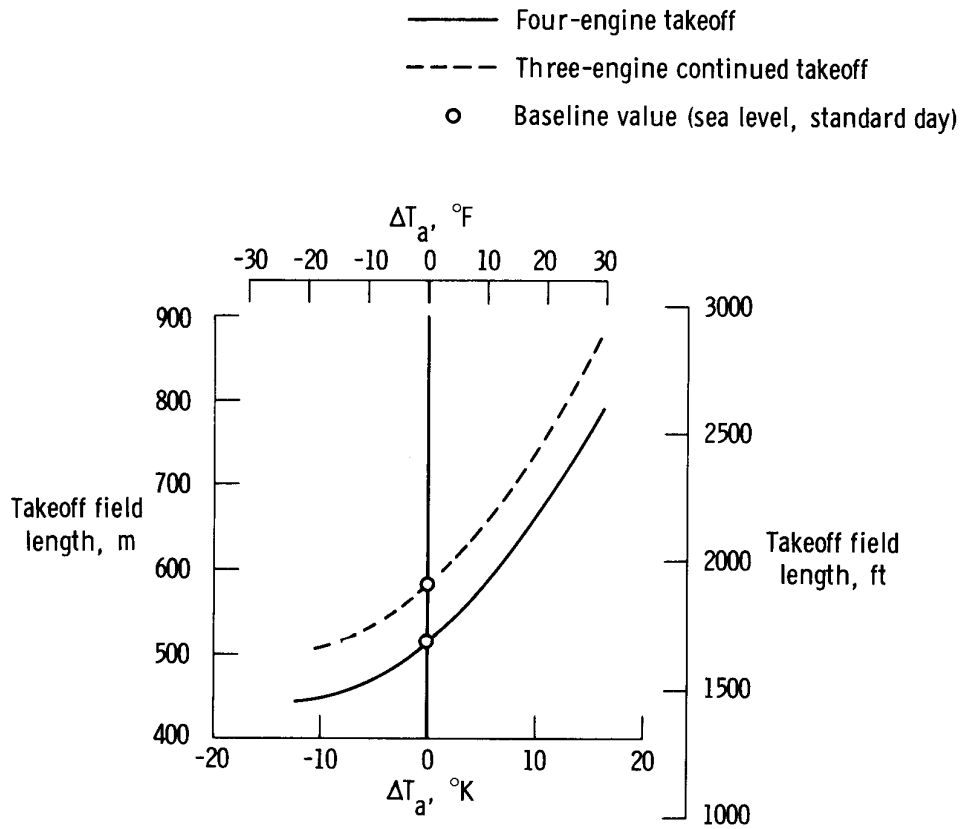

(a) Ambient temperature.

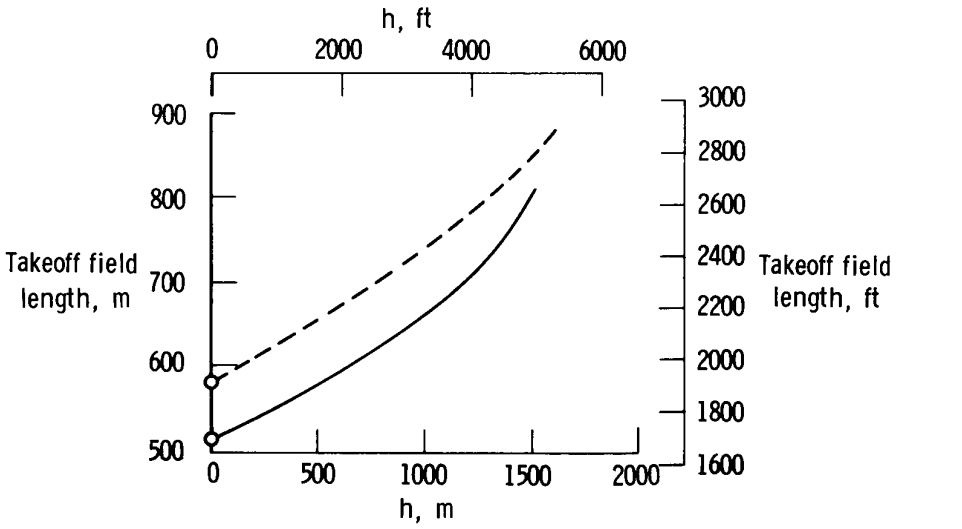

(b) Elevation.

Figure 9. Effect of ambient temperature and elevation on takeoff field length. 35° flaps.

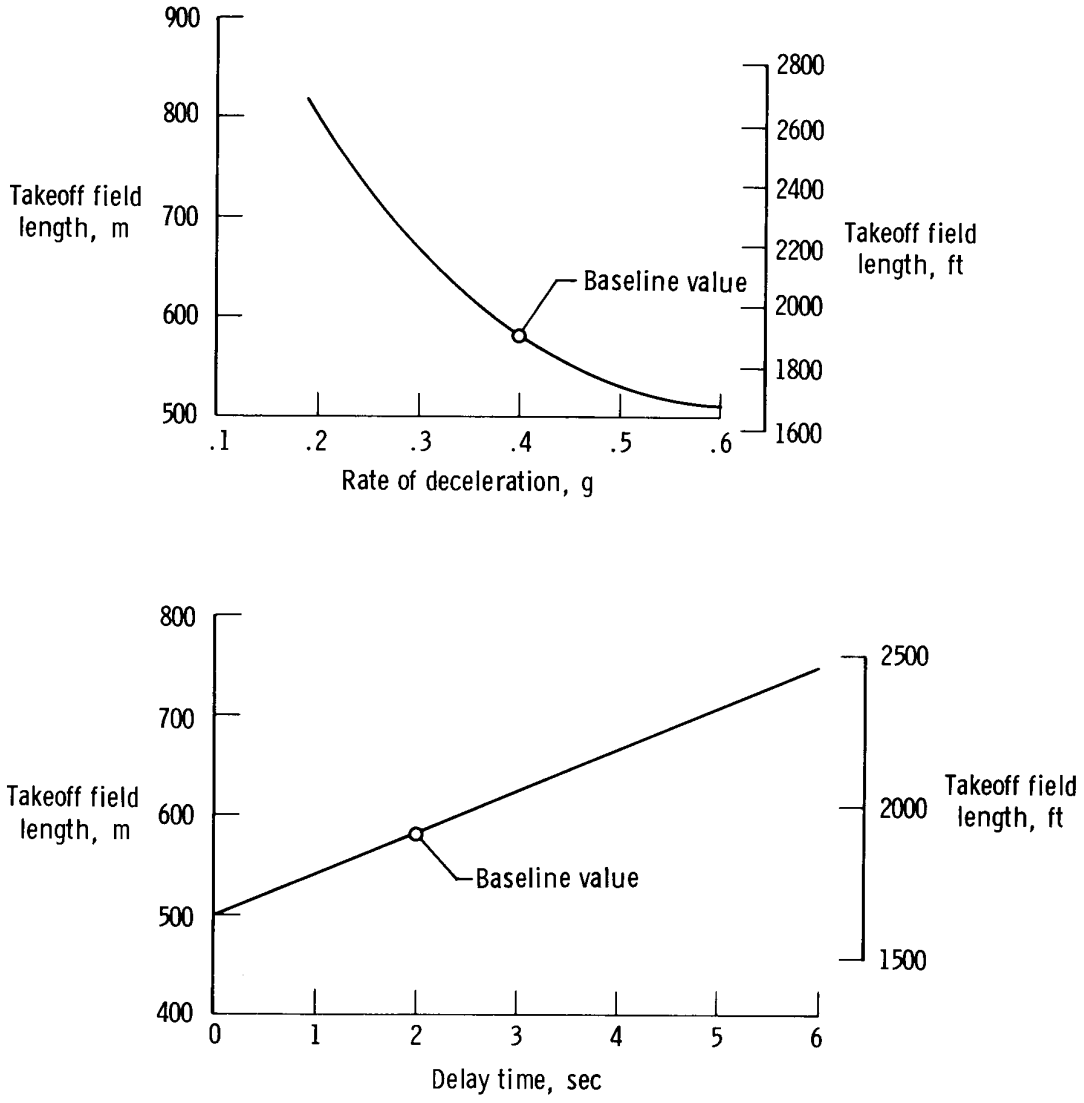

Figure 10. Effect of rollout deceleration rate and delay before braking on takeoff field length for the rejected takeoff maneuver. V_1 = 80.5 knots; 35° flaps.

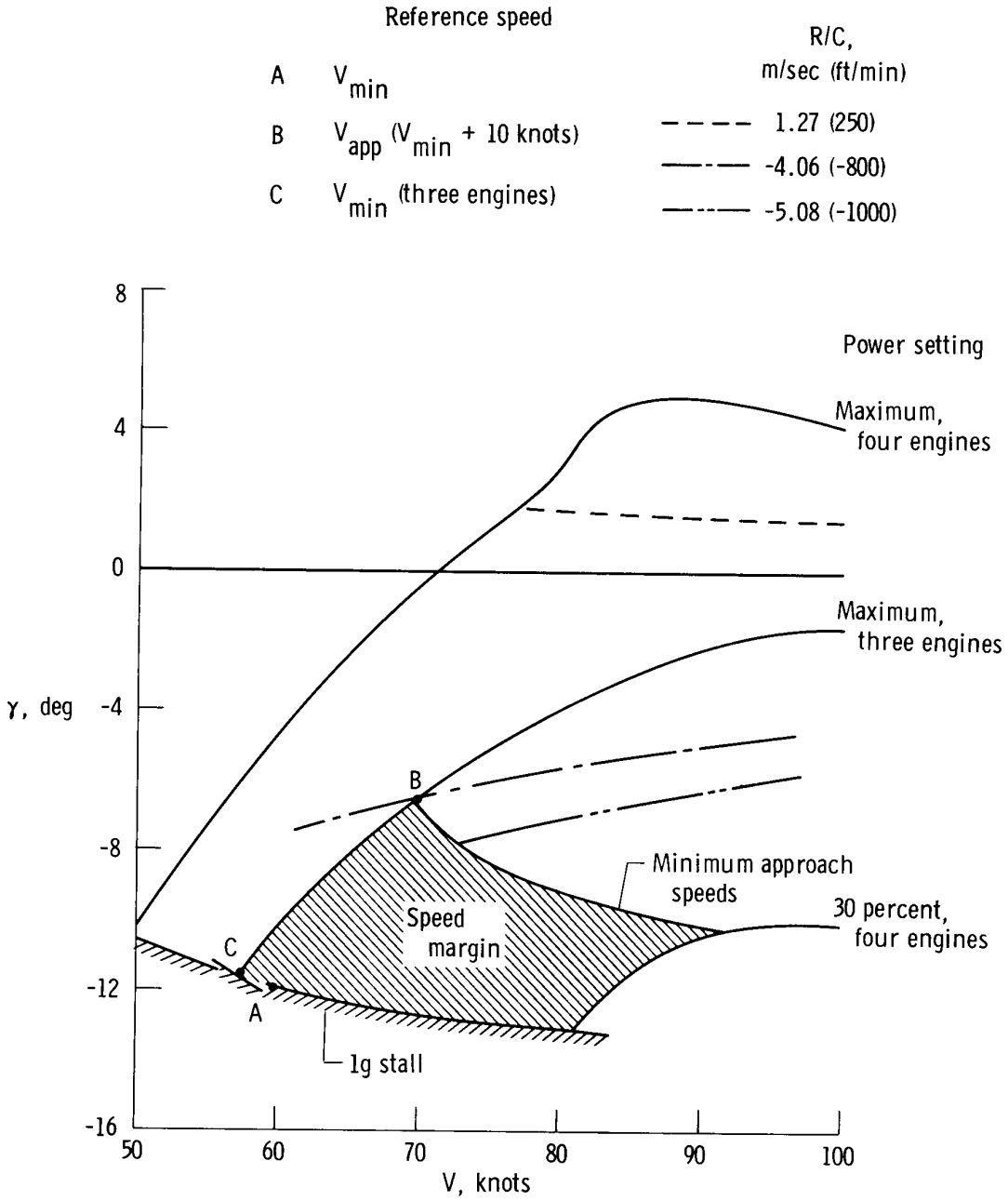

Figure 11. Operational envelope for landing. Baseline configuration; 60° flaps.

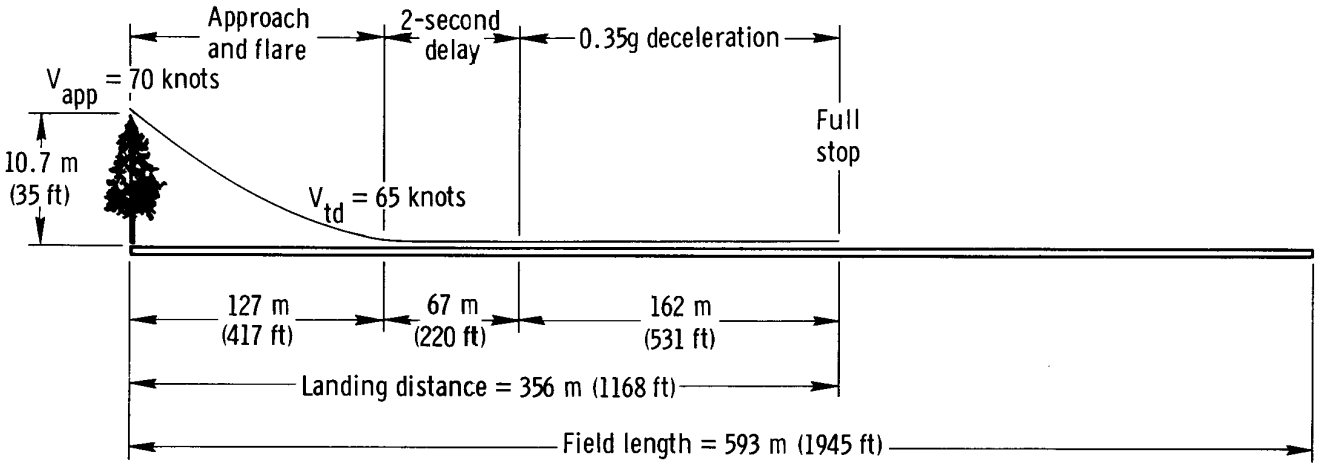

Figure 12. Landing performance. Baseline configuration; 60° flaps.

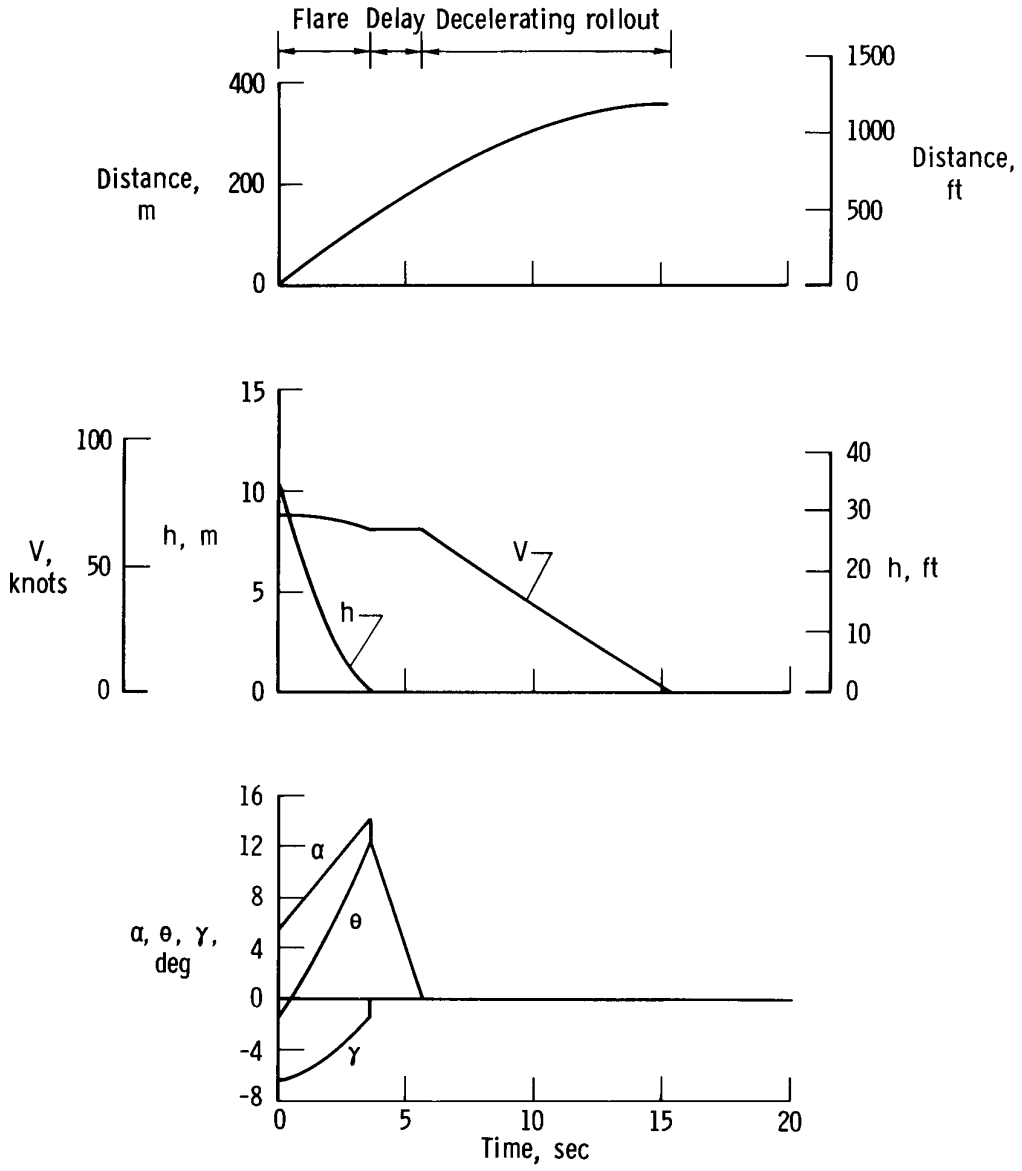

Figure 13. Time history of landing. Baseline configuration; 60° flaps.

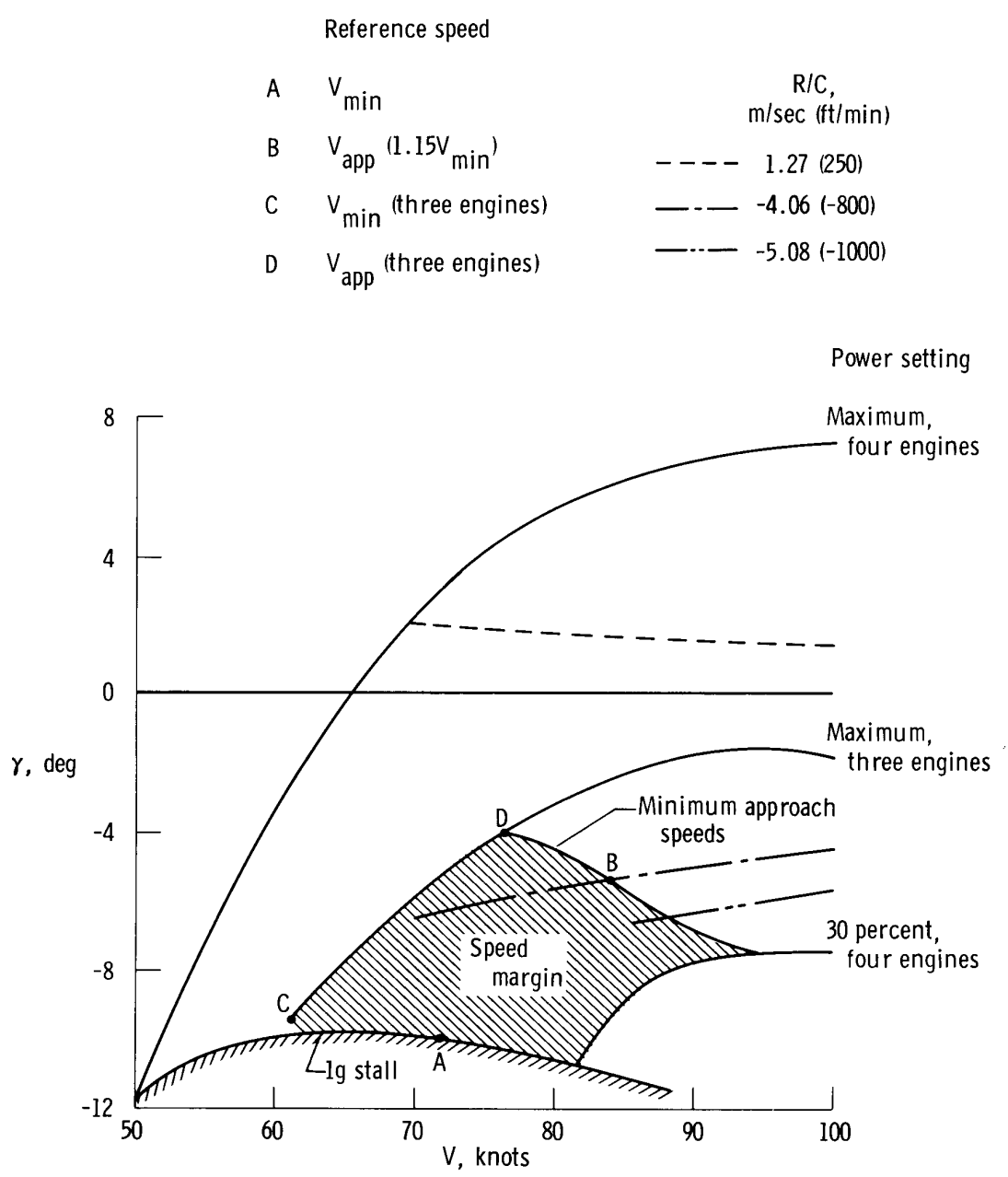

Figure 14. Operational envelope for landing. Baseline configuration; 50° flaps.

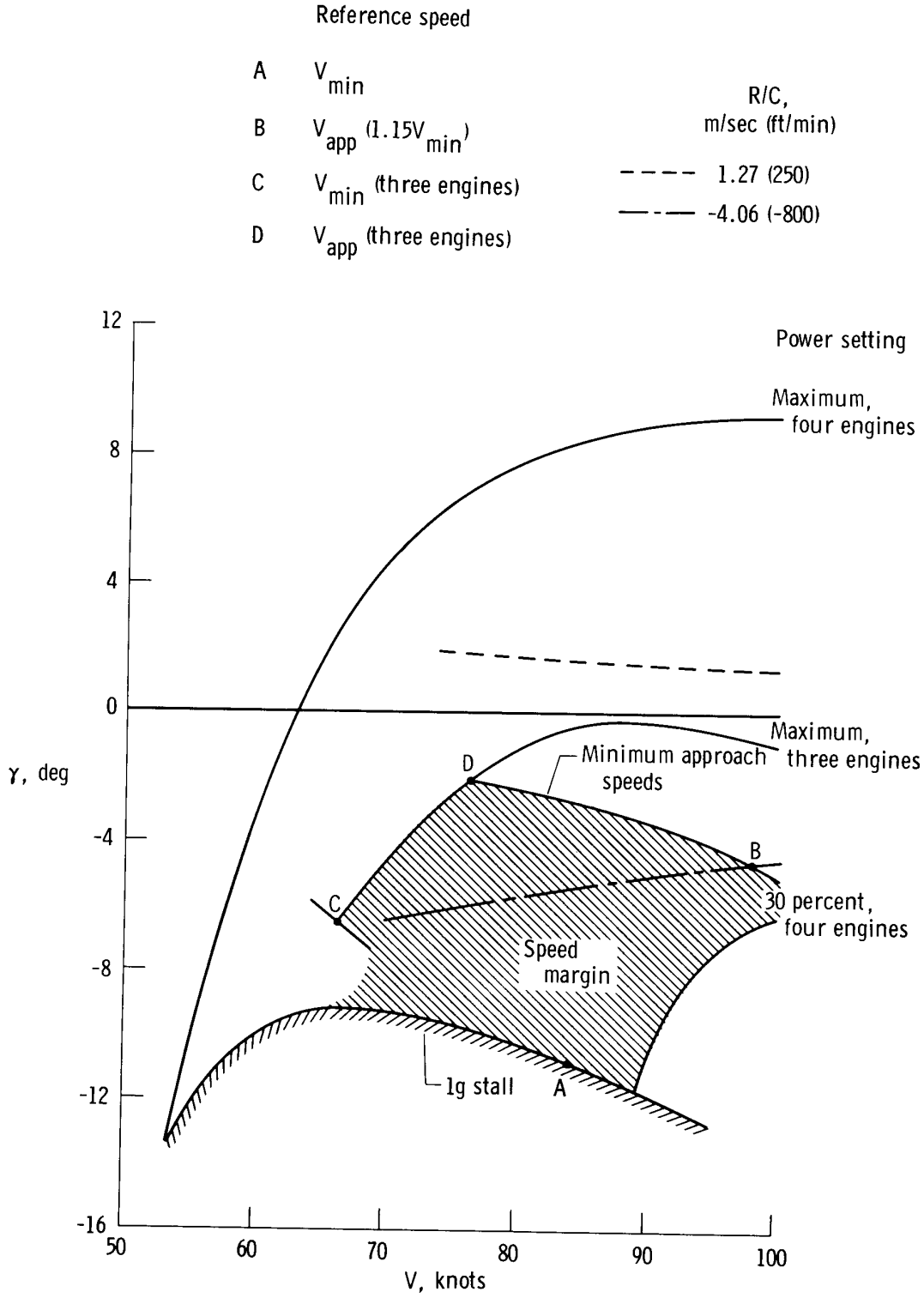

Figure 15. Operational envelope for landing. Baseline configuration; 40° flaps.

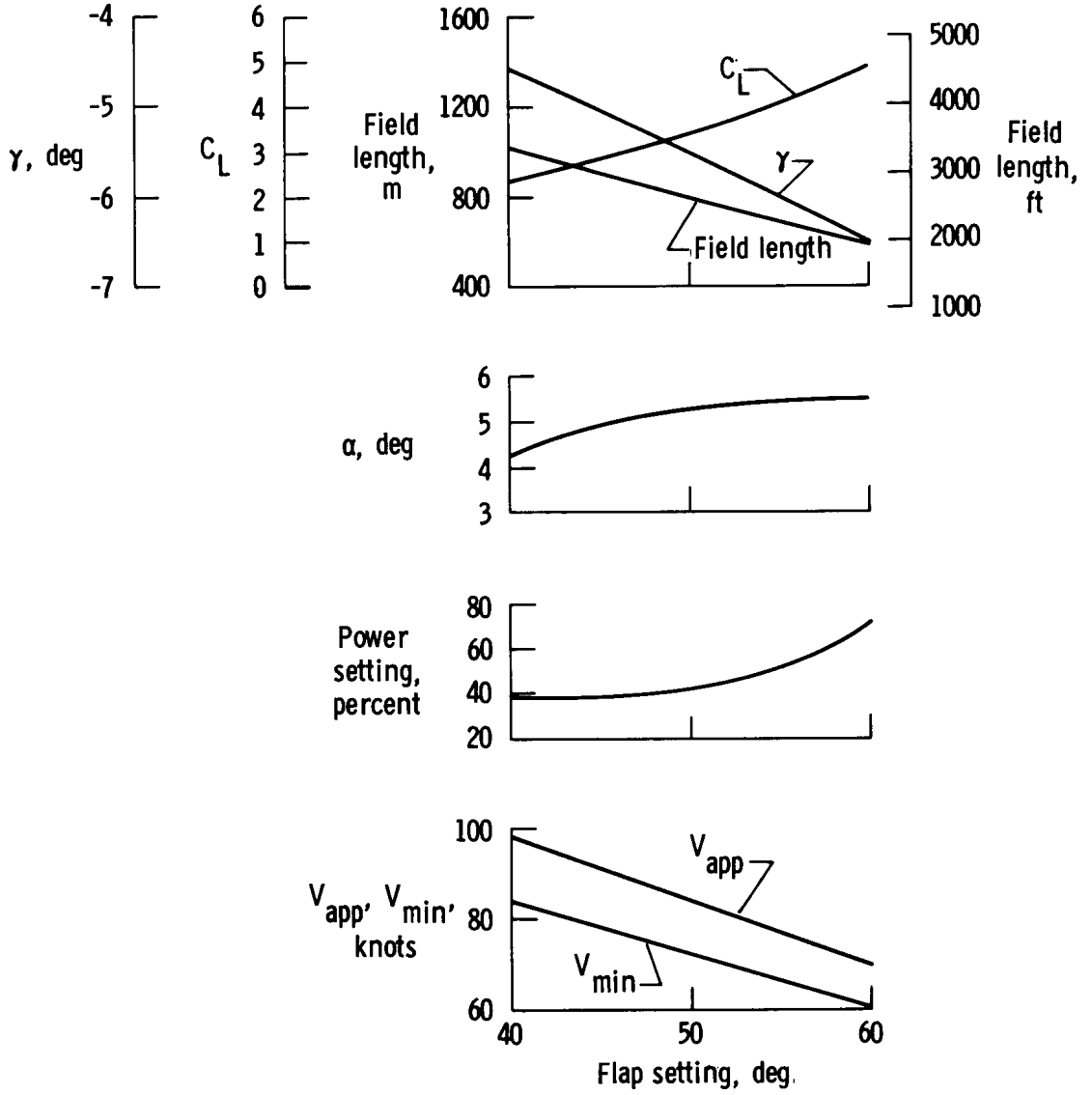

Figure 16. Variation of approach characteristics and performance with flap setting. Baseline configuration.

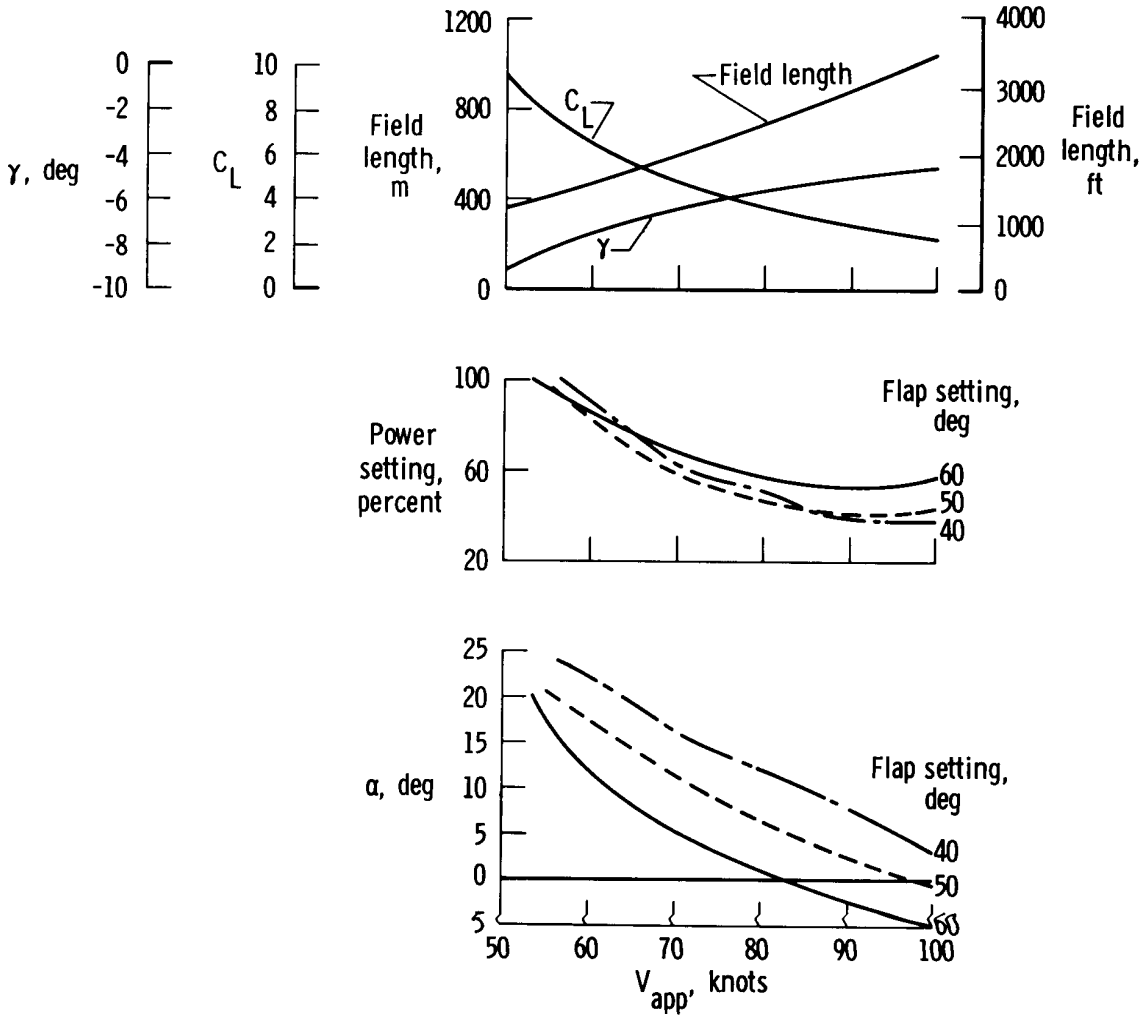

Figure 17. Comparison of 4.06-meter-per-second (800-foot-per-minute) descent characteristics for three flap settings. Baseline configuration.

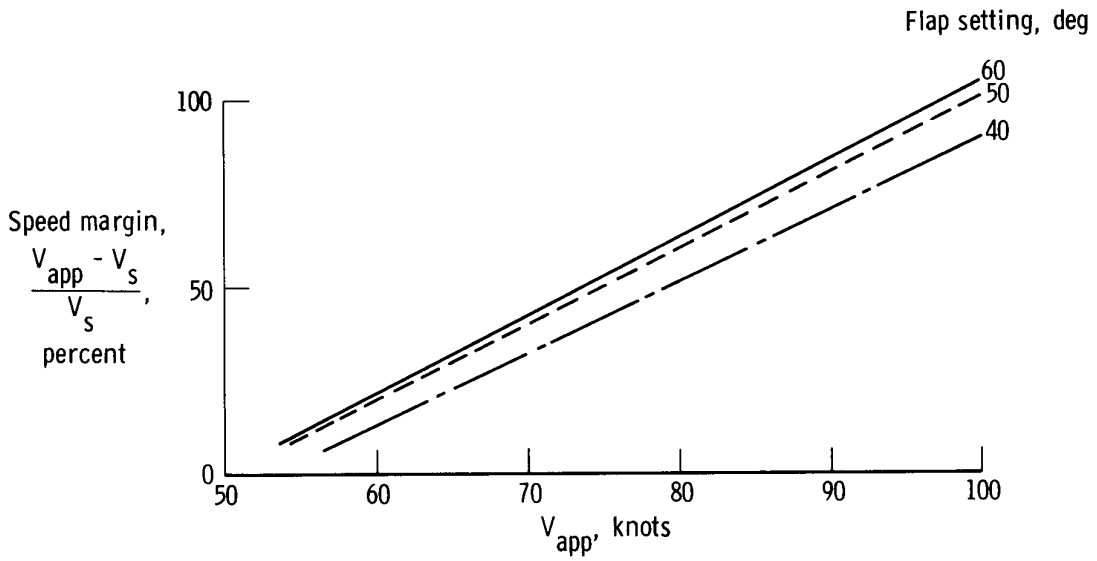

(a) Maximum power.

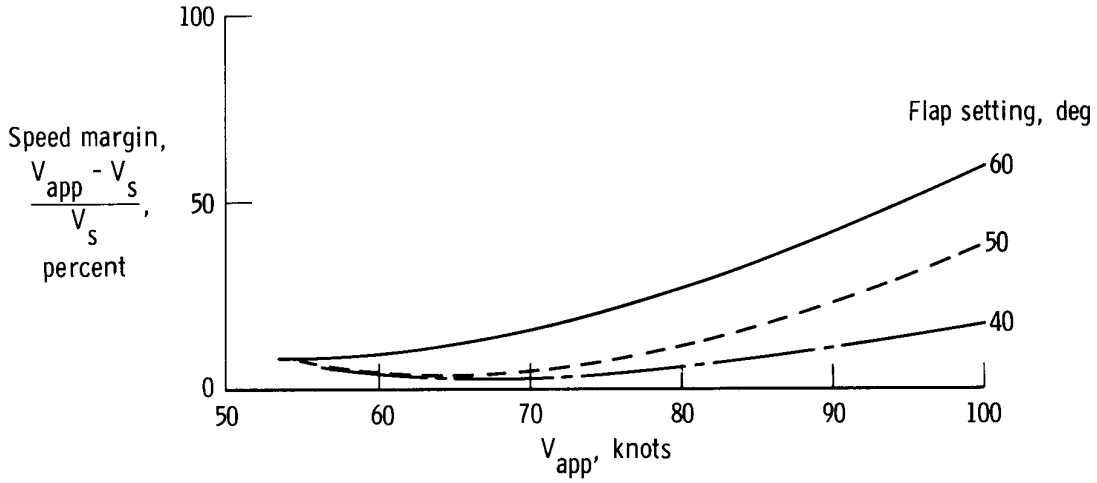

(b) Approach power.

Figure 18. Comparison of speed margins for a 4.06-meter-per-second (800-foot-per-minute) descent rate for three flap settings. Baseline configuration.

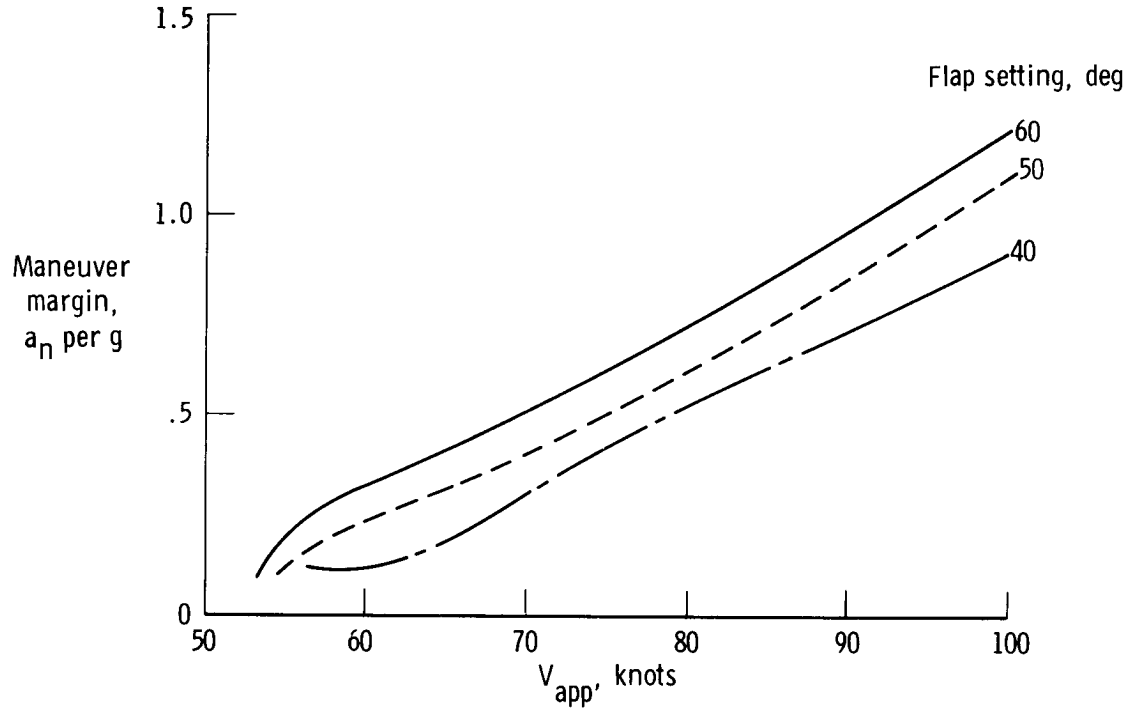

(a) Maximum power.

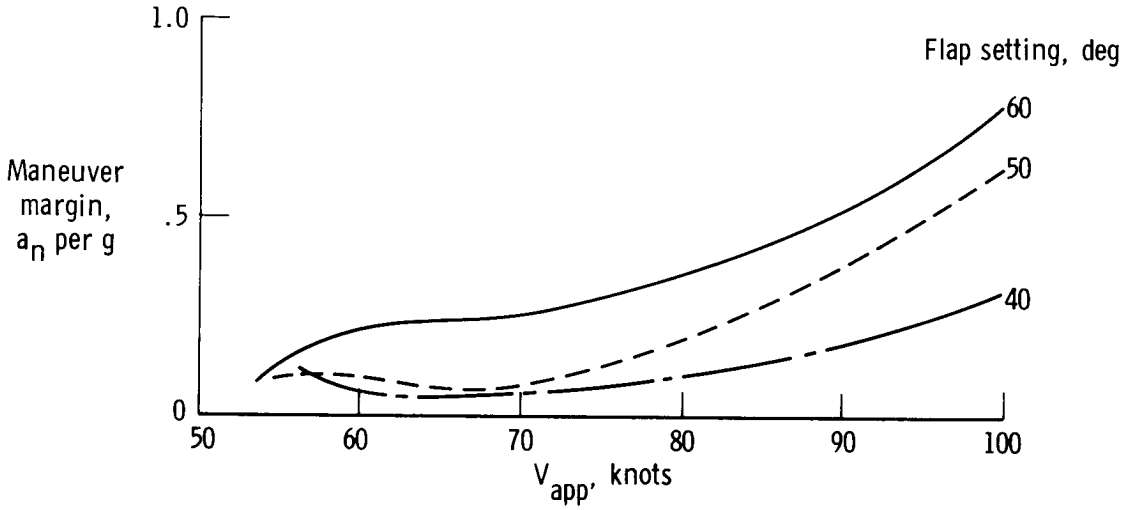

(b) Approach power.

Figure 19. Comparison of maneuver margins for a 4.06-meter-per-second (800-foot-per-minute) descent rate for three flap settings. Baseline configuration.

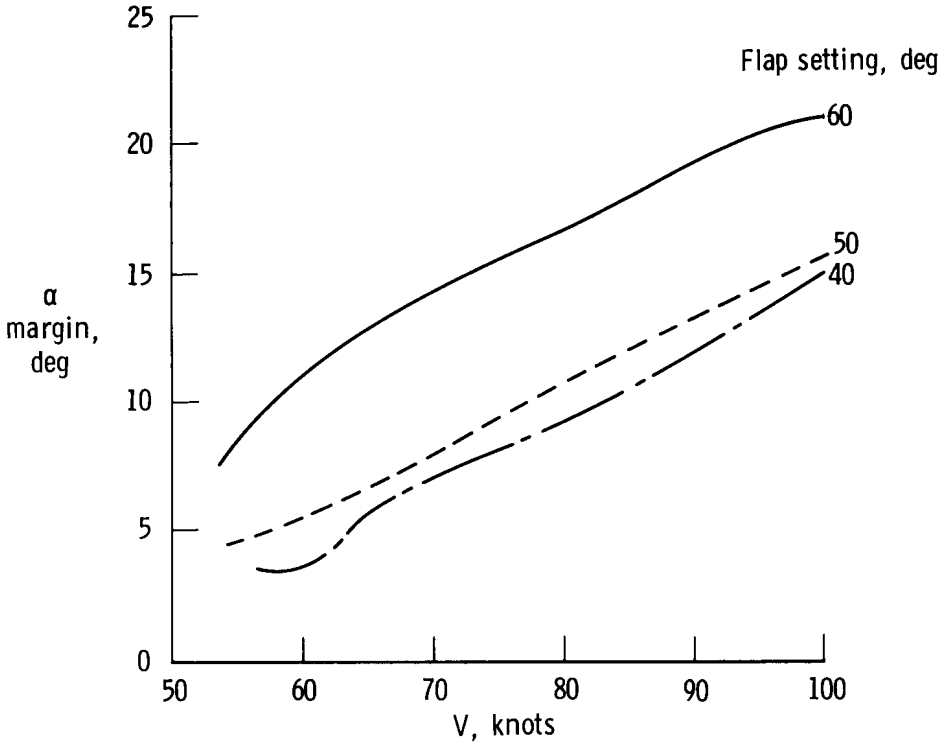

(a) Maximum power.

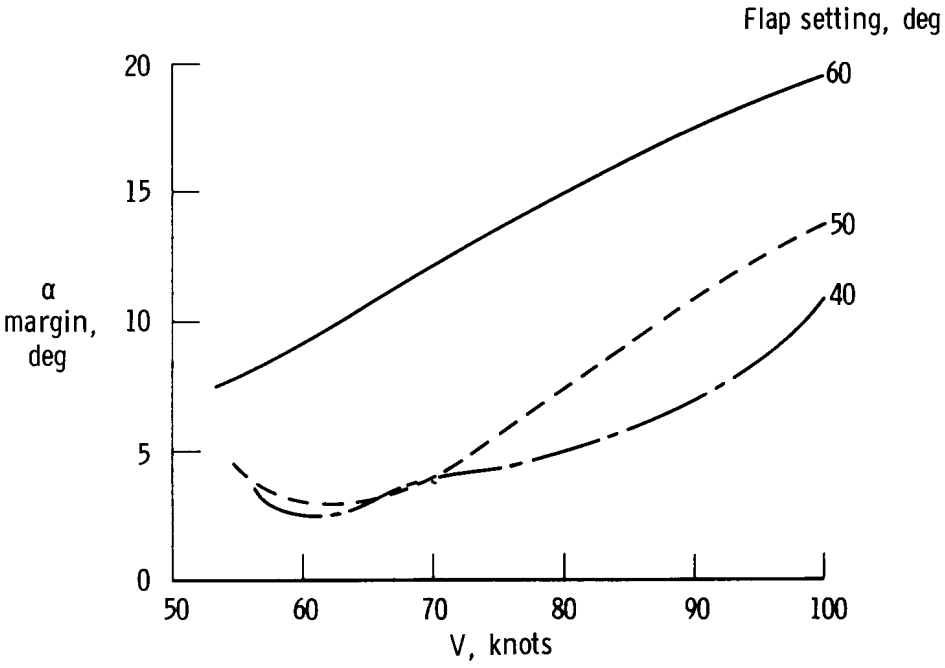

(b) Approach power.

Figure 20. Comparison of angle-of-attack margins for 4.06-meter-per-second (800-foot-per-minute) descent rate for three flap settings. Baseline configuration.

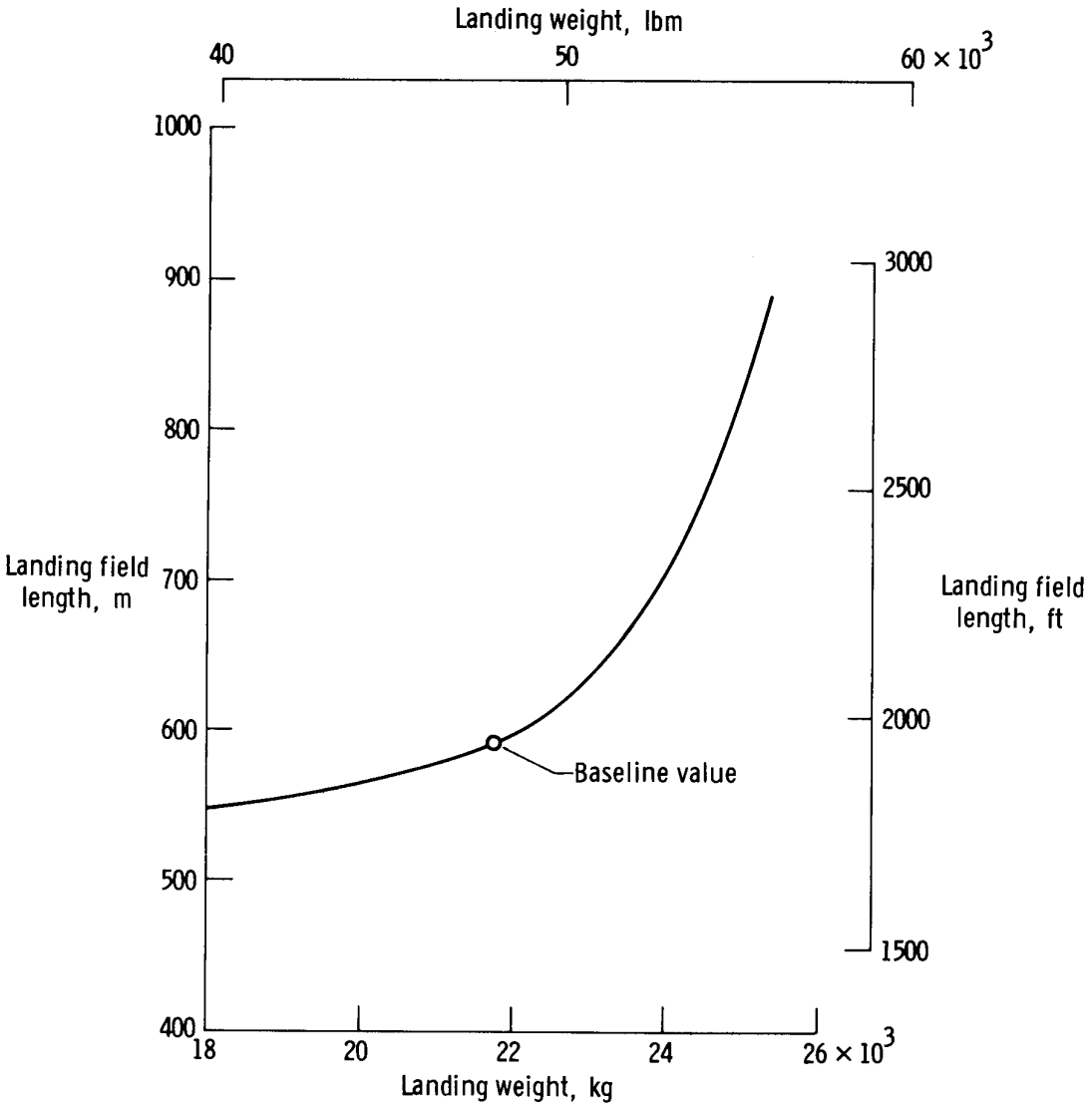

Figure 21. Effect of weight on landing field length. 60° flaps.

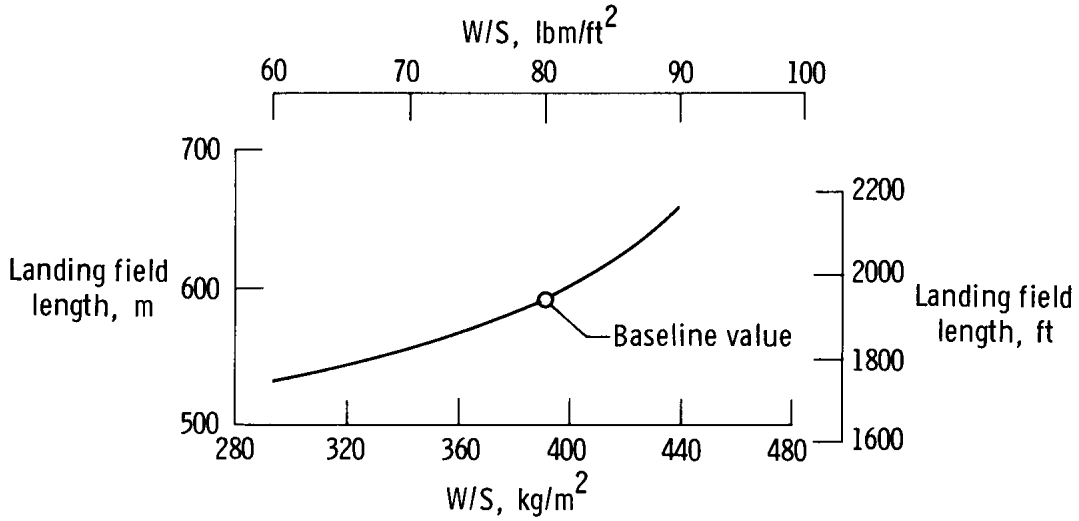

(a) Wing loading.

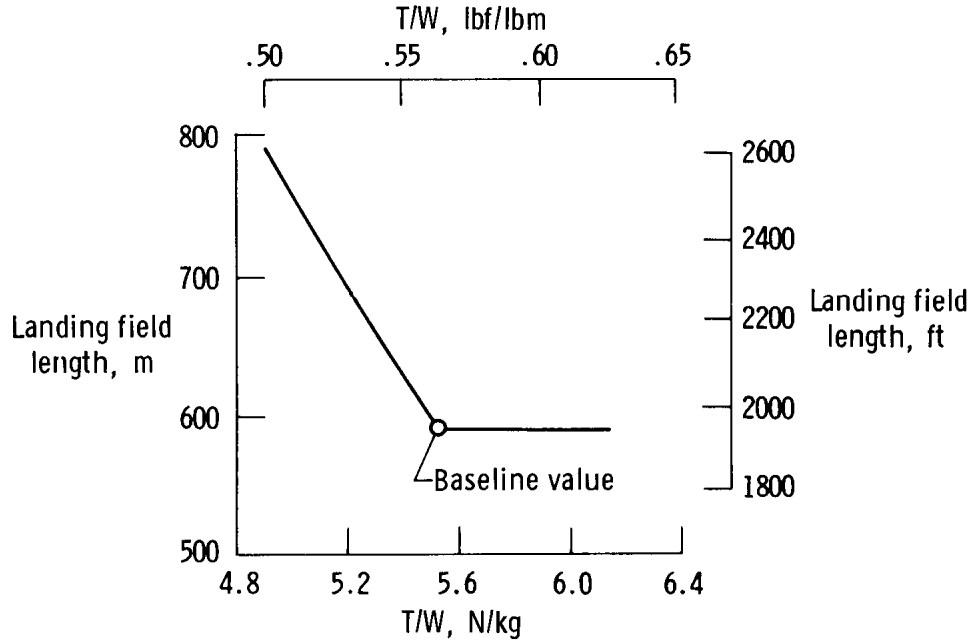

(b) Thrust-to-weight ratio.

Figure 22. Effect of wing loading and thrust-to-weight ratio on landing field length. 60° flaps.

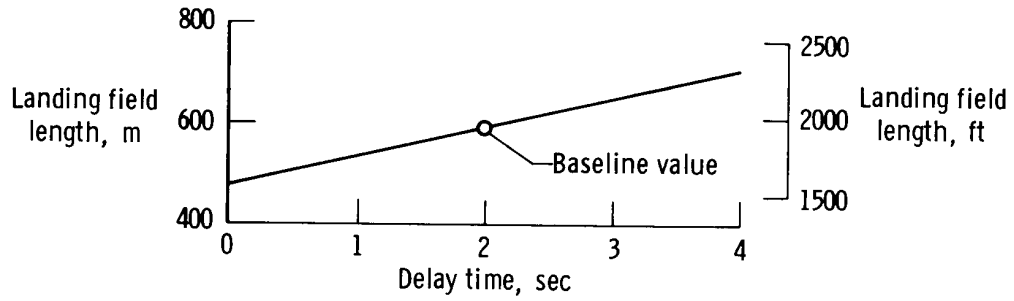

(a) Delay.

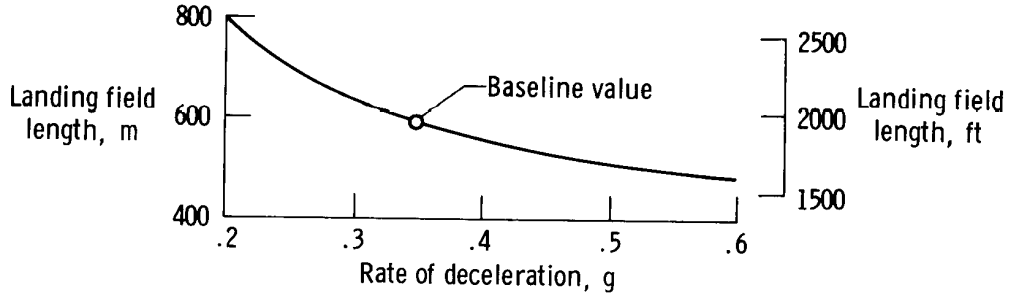

(b) Rate of deceleration during rollout.

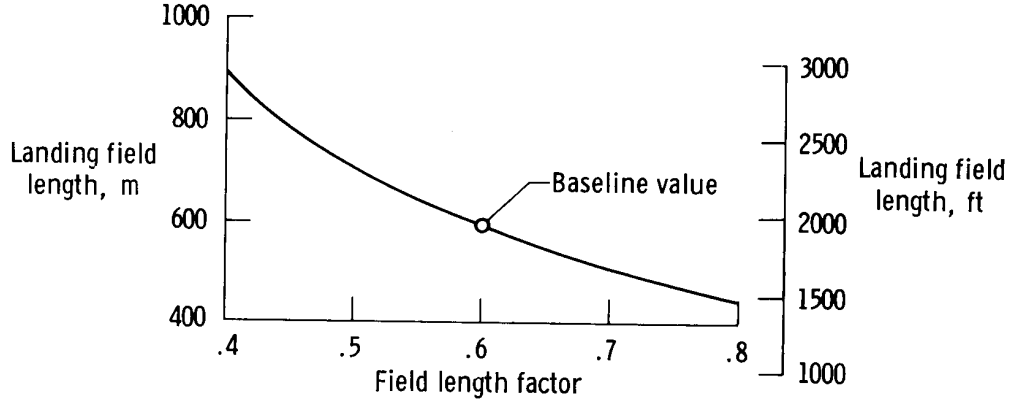

(c) Field length factor.

Figure 23. Effect of delay before braking, rollout deceleration rate, and field length factor on landing field length. V_{app} = 70 knots.

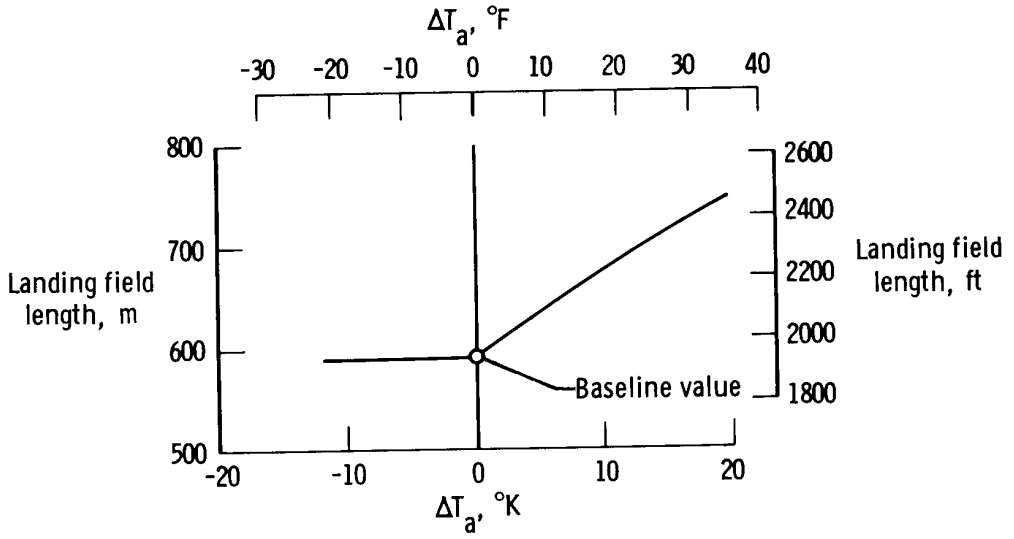

(a) Ambient temperature.

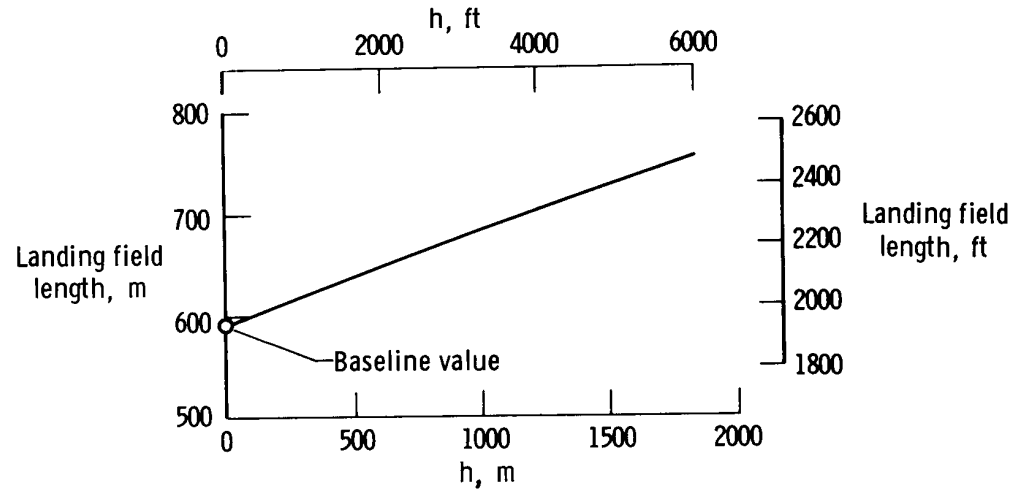

(b) Elevation.

Figure 24. Effect of ambient temperature and elevation on landing field length. 60° flaps.

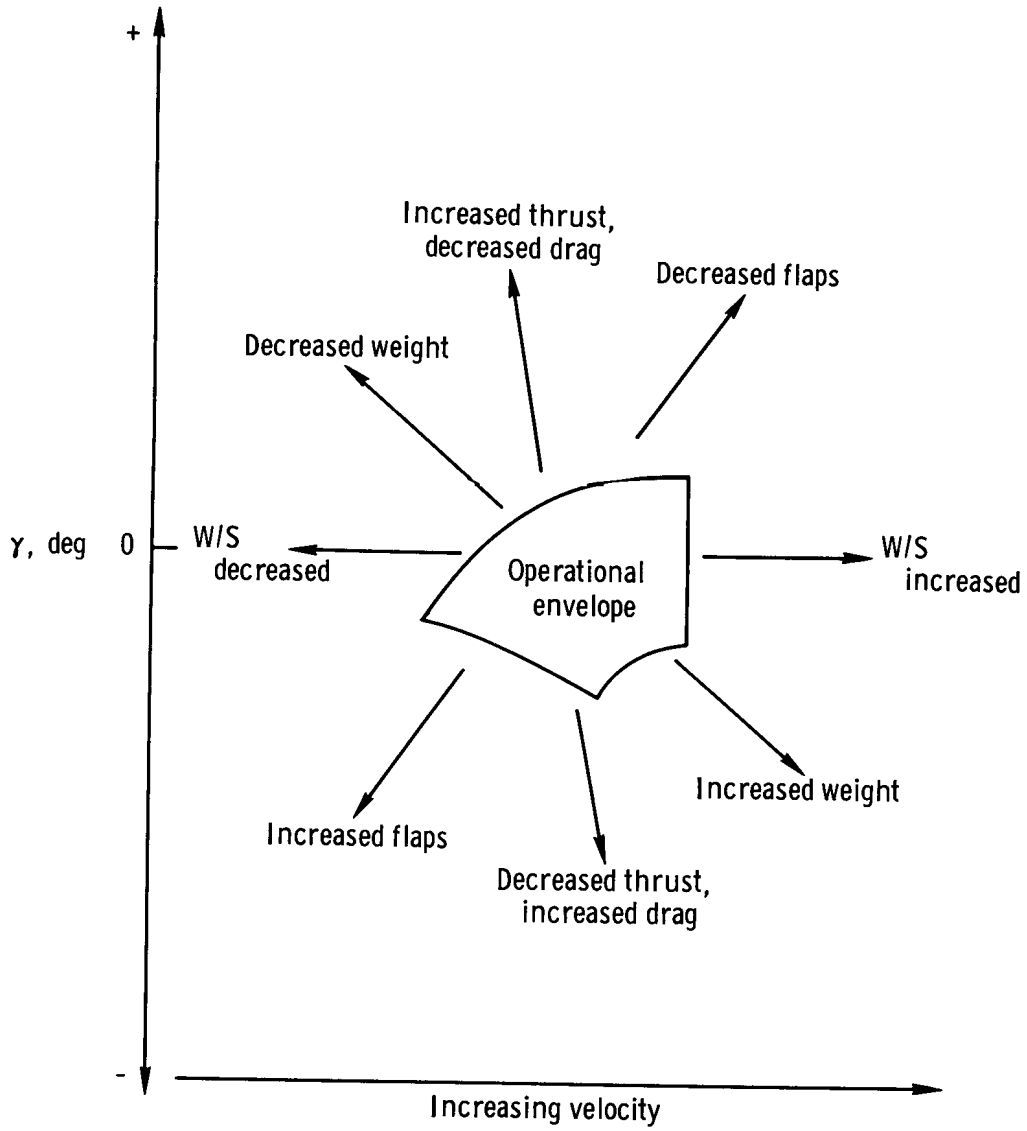

Figure 25. Factors that affect the position of the operational envelope.